molecular pharmaceutics

Editors' Choice

pubs.acs.org/molecularpharmaceutics

Review

Intelligent Design of Lipid Nanoparticles for Enhanced Gene Therapeutics

Published as part of Molecular Pharmaceutics special issue "Computational Methods in Drug Delivery".

Yichen Yuan,[#] Ying Li,[#] Guo Li,[#] Liqun Lei,[#] Xingxu Huang,[*] Ming Li,[*] and Yuan Yao[*]

Cite This: *Mol. Pharmaceutics* 2025, 22, 1142−1159

Read Online

ACCESS | Metrics & More | Article Recommendations

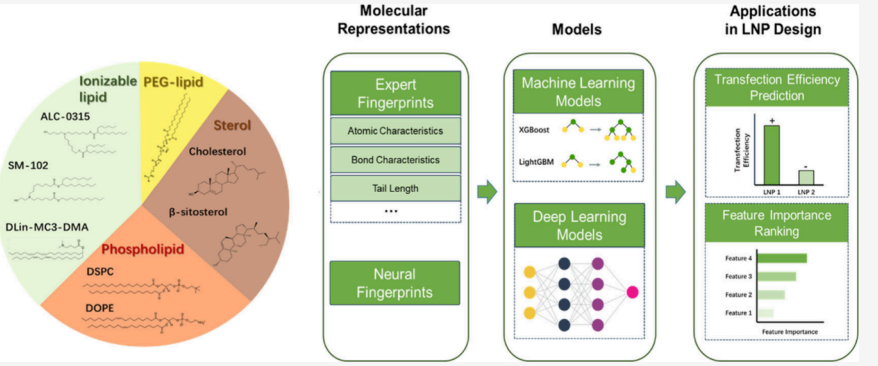

ABSTRACT: Lipid nanoparticles (LNPs) are an effective delivery system for gene therapeutics. By optimizing their formulation, the physiochemical properties of LNPs can be tailored to improve tissue penetration, cellular uptake, and precise targeting. The application of these targeted delivery strategies within the LNP framework ensures efficient delivery of therapeutic agents to specific organs or cell types, thereby maximizing therapeutic efficacy. In the realm of genome editing, LNPs have emerged as a potent vehicle for delivering CRISPR/Cas components, offering significant advantages such as high *in vivo* efficacy. The incorporation of machine learning into the optimization of LNP platforms for gene therapeutics represents a significant advancement, harnessing its predictive capabilities to substantially accelerate the research and development process. This review highlights the dynamic evolution of LNP technology, which is expected to drive transformative progress in the field of gene therapy.

KEYWORDS: *lipid nanoparticles, gene therapy, machine learning*

1. INTRODUCTION

The development of effective intracellular delivery methods has been a significant challenge in the field of gene therapeutics. Gene editing agents are typically delivered *in vivo* using either viral or nonviral approaches. Among these, adeno-associated virus (AAV) is the most widely used vector. Its popularity stems from its high efficiency in treating conditions that affect the eye, liver, muscles, and central nervous system.[1] However, several limitations may constrain its biomedical applications. First, AAV's limited packaging capacity presents a challenge for the inclusion of large gene editing agents.[2] Second, the prolonged expression of cargo by AAV in transduced cells could potentially result in off-target editing, which poses a risk in the context of genome engineering.[3] Third, the range of targetable tissues for AAV is relatively limited,[1] and it may elicit an immune response, carrying the risk of viral genome integration.[4] Considering these challenges, nonviral delivery systems are emerging as viable alternatives for gene-editing therapies.

Lipid nanoparticles (LNPs) represent a highly promising nonviral delivery platform for a variety of therapeutic nucleic acids, including short interfering RNA (siRNA), mRNA (mRNA), single-guide RNA (sgRNA), and plasmid DNA (pDNA).[4] The synthetic nature of LNPs enables precise control through the adjustment of lipid composition and manipulation of other parameters, and they also have the potential for targeted delivery to a wide range of cells and tissues, either by utilizing their inherent surface characteristics or through the strategic conjugation of specific ligands.[5−8]

Received: August 16, 2024
Revised: January 1, 2025
Accepted: January 2, 2025
Published: January 29, 2025

https://doi.org/10.1021/acs.molpharmaceut.4c00925
Mol. Pharmaceutics 2025, 22, 1142−1159

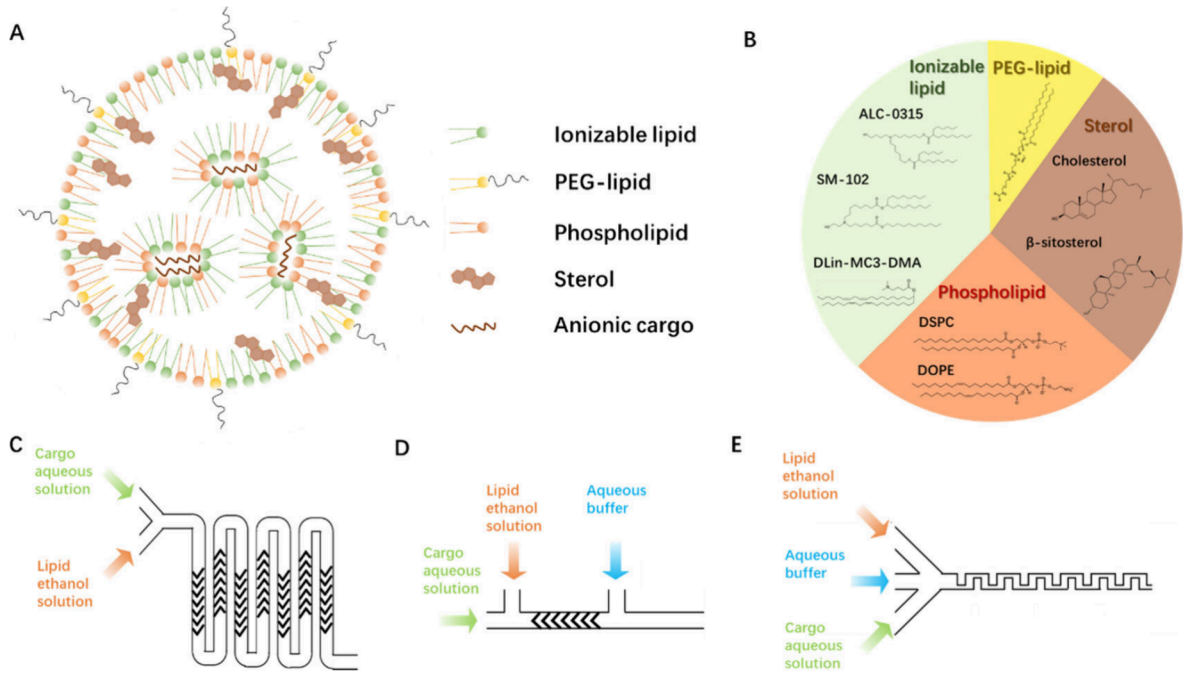

Figure 1. (A) LNP consists of four lipid components that enable encapsulating varied anionic cargos. (B) Lipid molecules applied in LNP formulation. (C) Two-inlet microfluidic device with herringbone geometry.[9] (D) Three-inlet microfluidic device with herringbone geometry encapsulating siRNA by LNP.[10] (E) The three-inlet microfluidic device used to produce RNP-LNP efficiently preventing aggregation.[11]

Machine learning has the potential to revolutionize the design of LNPs by predicting the efficiency of novel formulations and providing insights into delivery mechanisms. This capability allows for the rapid screening of a wide array of LNP formulation candidates. In this review, we provide an overview of the formulation and fabrication processes of LNPs, along with targeted delivery strategies. We explore the application of LNPs in CRISPR/Cas therapies and discuss the optimization of LNPs facilitated by machine learning. The review highlights the advancements and the untapped potential of this LNP delivery system.

2. FORMULATING LNPS FOR THERAPEUTIC GENOME EDITING

2.1. Structures and Components of LNPs. LNPs typically consist of four fundamental components: ionizable lipids, polyethylene glycol (PEG)-lipids, phospholipids, and sterols (as shown in Figure 1A,B). This formulation has been successfully employed in the FDA-approved siRNA therapy, Onpattro, and has been extensively used in mRNA vaccines during the COVID-19 pandemic.

2.1.1. Ionizable Lipid. Classical ionizable lipids consist of a hydrophilic amine headgroup, a linker, and a hydrophobic tail domain. The amine headgroup is ionizable, exhibiting positive charges below its pK_a, while the charge decreases when the pH exceeds the pK_a due to deprotonation. Most LNP studies focus on the apparent pK_a of the LNP rather than the intrinsic pK_a of the ionizable lipid, as the apparent pK_a reflects the ionization status of all molecules within the LNP.[12] A previous study reported that the theoretical pK_a of individual ionizable lipid is 2−3 units higher than the apparent pK_a of LNP containing the corresponding ionizable lipid.[13] For reading convenience, the term "pKa value" mentioned in the following section refers to the apparent pK_a of LNP unless otherwise specified. To enhance the design of LNPs, it is essential to engineer ionizable lipids to exhibit pK_a below 7. This approach endows LNP with minimal charges under physiological conditions (pH ≈ 7.4), reducing overall toxicity and blood clearance after intravenous (IV) injection. In an acidic environment, ionizable lipid will be cationic, which is pivotal for encapsulating the anionic nucleic acid cargo. The positive charges displayed on ionizable lipid also facilitates the release of cargo from the acidic endosomal compartment by disrupting the anionic endosomal membrane.

However, lipids with a pK_a value that is too low may exhibit insufficient interactions with the negatively charged endosome lumen.[14] Studies have shown that ionizable lipids with a pK_a below 5.5 are ineffective for liver-specific siRNA delivery.[15] Apart from pK_a, the efficacy of LNPs is influenced by their tendency to form nonbilayer structures, such as the inverted hexagonal phase (H_{II}). Ionizable lipids with high potency, exemplified by DLin-KC2-DMA (KC2, pK_a = 6.68), which possess a 'cone-shaped' molecular structure, have demonstrated the ability to induce H_{II} phase transformation in the endosomal membrane. This property results in superior *in vivo* efficacy compared to conventional lipids like DLinDMA.[16] The optimal pK_a range for IV delivery systems is between 6.2 and 6.5, highlighting DLin-MC3-DMA (MC3, pK_a = 6.44) as the most potent lipid for hepatocyte gene silencing.[17] MC3 has emerged as a benchmark ionizable lipid in a variety of nucleic acid delivery systems, including the commercial product Onpattro.[14]

The route of administration also impacts the efficiency of LNPs *in vivo*. Studies have indicated that while MC3 is superior for IV injection, KC2 exhibits higher efficacy *in vitro* and *in vivo* following intramuscular (IM) injection due to its 'cone-shaped' structure.[13] However, LNPs formulated with MC3 have been observed to produce extended local and systemic exposure following IM administration, potentially leading to adverse clinical effects.[18] Moderna's LNP, composed

https://doi.org/10.1021/acs.molpharmaceut.4c00925
Mol. Pharmaceutics 2025, 22, 1142−1159

of lipid SM-102 (Lipid H, pK_a = 6.68), has shown improved biodegradability and mRNA expression compared to MC3-based LNPs after IM injection.[18] This LNP has been utilized in the vaccine Spikevax.

pH-responsive polymer−lipid hybrid materials, such as 7C1 (lipid tail-modified poly(ether imide), pK_a ∼ 5.0) can specifically target siRNA delivery to lung endothelial cells.[19] Bioreproducible lipids provide a viable alternative for the formulation of biodegradable LNPs, functioning via a distinct mechanism compared to conventional ionizable lipids. These reproducible LNPs remain stable in physiological conditions, and yet they undergo degradation in the cytosol through a disulfide bond exchange mechanism, promoting the intracellular release of gene editing agents.[20] It has been reported that LNPs based on reproducible lipids were more efficient in delivering Cas9 mRNA and sgRNA than those based on DLin-MC3-DMA.[21]

2.1.2. PEG-lipid. The incorporation of PEG-lipids onto the LNP surface can shield the positive charge, extending the circulation lifetime and preventing aggregation through steric hindrance.[22] PEG-lipids consist of a PEG chain conjugated to an alkyl chain via phosphate, glycerol, or other linkers.[23] In nebulized LNP therapies, manipulating the quantity and structure of PEG-lipids could improve LNP stability thereby enhancing the delivery efficiency.[24] For IV-administered LNPs, PEG-lipids dissociate over time, leaving the ionizable LNP available for transfection.[25] *In vitro* studies have shown that PEG-lipids with shorter alkyl chains dissociate more rapidly, allowing for quicker LNP activation and cell association.[26] On the other hand, *in vivo* research reported that LNPs with shorter alkyl chains are cleared more quickly from the bloodstream, whereas longer chains enhance stability and facilitate bypass of the first-pass organs (e.g., liver, spleen, and lung) to reach targeted tumor sites.[25] However, the long alkyl chains may not be advantageous for targeted delivery systems, as they can hinder the formation of the protein corona.[27] This inhibition could potentially compromise the specificity of LNP delivery.

2.1.3. Sterol. Sterols are vital in mediating the structure of LNPs and enhancing encapsulation efficiency,[28] where cholesterol is the most common choice in LNP formulation. Cholesterol stabilizes LNPs by occupying interlipid tail spaces and maintaining a balance between fluidity and condensation of the lipid bilayer.[29] Other naturally occurring sterols are also occasionally incorporated into LNP formulations. For instance, β-sitosterol has demonstrated potential in enhancing endosomal escape and facilitating mRNA transfection in natural killer cells.[30]

2.1.4. Phospholipid. Phospholipids are strategically positioned on the LNP surface to promote bilayer phase formation[31,32] and mediate RNA loading into LNPs.[33] 1,2-Stearoyl-*sn*-glycerol-3-phosphocholine (DSPC) and 1,2-Dipalmitoyl-*sn*-glycerol-3-phosphoethanolamine (DOPE) are the most widely used phospholipids in LNP formulations. Anderson's lab found that DOPE is more efficient than DSPC in mRNA delivery due to its tendency to form H_{II} phases upon fusion with the endosomal membrane, which destabilizes the membrane and facilitates endosomal escape.[34] Recently, the optimization of phospholipids has emerged as a promising method for enhancing LNP delivery systems. LNPs formed with 1,2-Dioleoyl-*sn*-glycerol-3-phosphocholine (DOPC) exhibited higher efficacy than both DSPC and DOPE. DOPC's quaternized amine headgroup and unsaturated lipid tail promote endosomal escape through strong proton sponge effects and increased membrane fluidity, respectively.[21] The phospholipid 9A1P9, demonstrated 40- to 965-fold higher *in vivo* efficacy than DOPE and DSPC, highlighting the importance of H_{II} phase formation in phospholipid efficacy.[35]

2.2. Fabrication of LNPs via Microfluidic Systems. The LNP fabrication studies involved the encapsulation of nucleic acids by trapping siRNA within preformed liposome vesicles through rapid mixing processes.[36] Subsequently, stepwise mixing technology was developed, which involved the combination of DNA aqueous solutions with lipid ethanol solutions in a T-shaped mixing chamber, followed by a stepwise dilution.[37] However, these methods often resulted in LNPs with high polydispersity and inconsistent batch-to-batch reproducibility, primarily due to uncontrolled mixing conditions.[10]

Microfluidics has emerged as a technological advancement for the fabrication of liposomes and LNPs. The scalability of this manufacturing process is enhanced through the parallelization of mixing devices. Critical parameters for controlling LNP formation include the residence time within the mixing chamber and the geometrical design of the microfluidic mixer.[9] Droplet microfluidic devices utilize two immiscible fluids to fabricate liposome vesicles, where water is pumped into an oil-surfactant mixture flow, and vesicles are formed due to shear forces perpendicular to the oil-surfactant flow generated by the water.[38] Microfluidic system based on the hydrodynamic focusing of two miscible fluids (e.g., isopropanol and acidic aqueous buffer) was capable of producing smaller liposomes compared to the droplet microfluidic devices.[39,40] Liposomes formed along the aqueous/alcohol interfacial phase where the lipid solubility was reduced, which induced the self-assembly of lipids into planar lipid bilayers. These bilayers subsequently closed into spherical vesicles due to surface tension effects.[40] After LNP formation, dialysis is often employed to remove residual ethanol and achieve pH neutralization. As the pH is adjusted to neutral, the fusion of small vesicles into larger vesicular structures can be observed.[31]

The incorporation of a staggered herringbone pattern into microfluidic devices has been shown to increase throughput, a design feature implemented in many microfluidic LNP formation systems (Figure 1C).[9] The herringbone geometry within the microfluidic channel induces chaotic flow, leading to rapid and effective mixing of the components and homogeneous nucleation of nanoparticles. While most microfluidic systems are designed with two inlets, LNPs have also been prepared using three-inlet devices to enhance functionality. Suzuki et al. developed a microfluidic device featuring a third inlet that introduces an aqueous buffer at the junction of the other two inlets, aiming to prevent the aggregation of ribonucleoprotein (RNP) cargo (Figure 1E).[11] Anderson's laboratory further refined the microfluidic system by adding an additional inlet for the injection of aqueous buffer post-LNP formation, which not only neutralized pH but also mitigated LNP aggregation (Figure 1D).[10]

2.3. Tailoring LNP Formulation Parameters. *2.3.1. Size.* The LNP size and its distribution are critical determinants for efficient gene delivery. Particle size significantly influences tissue penetration, clearance rates, and the mechanism of endocytosis. LNPs with a diameter of approximately 120 nm are primarily internalized through nonselective fluid-phase endocytosis, while smaller LNPs (less than 80 nm) might be

https://doi.org/10.1021/acs.molpharmaceut.4c00925
Mol. Pharmaceutics 2025, 22, 1142−1159

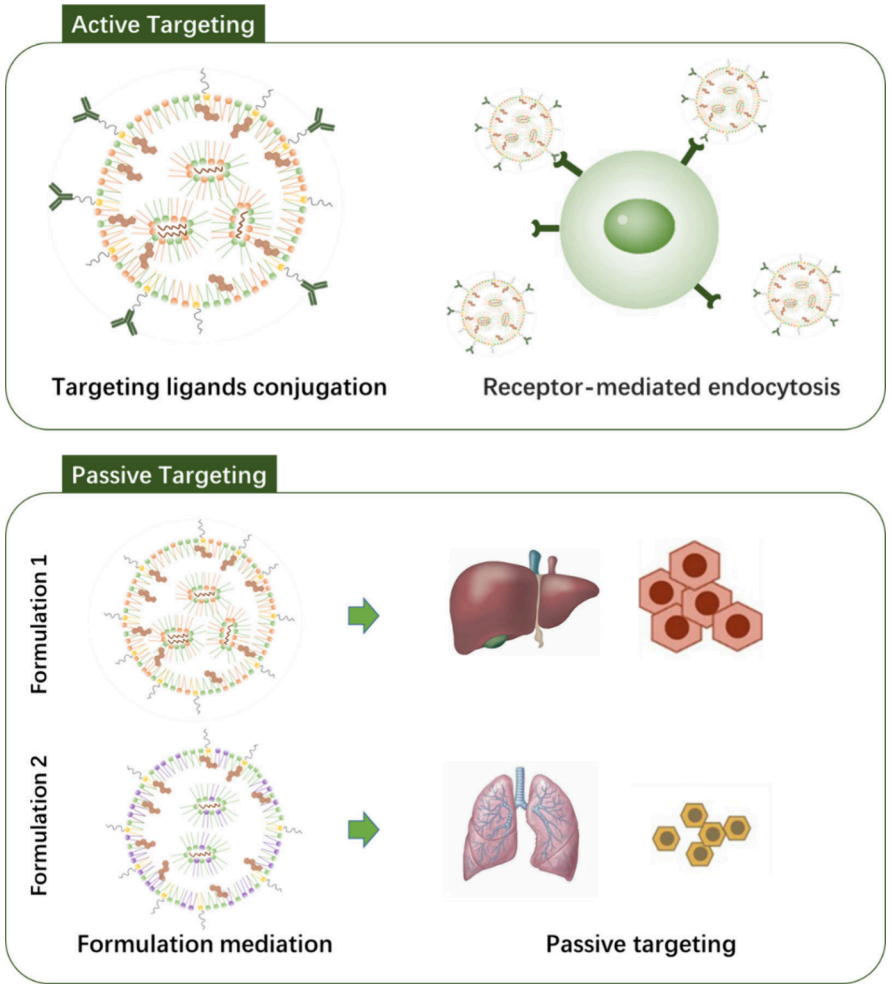

Figure 2. LNP targeted delivery enabled by active or passive targeting.

internalized via receptor-mediated endocytosis.[41] This size-dependent internalization pathway is crucial for the cellular uptake and subsequent intracellular trafficking of LNPs. There is a negative correlation between LNP size and permeation, with the optimal size being dependent on the target site. For hepatocyte targeting, LNPs should be smaller than liver endothelial fenestrations (100−150 nm), and smaller sizes correlate with increased transfection efficiency.[42] LNPs with sizes similar to the fenestrations risk being taken up by liver sinusoidal endothelial cells (LSECs), potentially hindering their interaction with hepatocytes.[43] For tumor-targeted delivery, sub-100 nm particles are preferred due to the smallest tumor model pore size being 100−200 nm.[44] However, very small LNPs, such as those around 30 nm, may not achieve high potency despite their enhanced permeability; they are cleared rapidly from the bloodstream and exhibit reduced *in vivo* efficacy due to rapid lipid dissociation and a limited nucleic acid payload.[27,45,46]

Microfluidic devices offer precise control over the size of LNPs. A rapid flow rate typically results in smaller LNPs, since it allows little time for self-assembling planar lipid fragments to grow before closing into the vesicle.[10] Elevating aqueous/alcohol flow rate ratio was also reported to reduce the LNP size.[47] Importantly, the geometry of the microfluidic channel, specifically its cross-sectional area, influences the size distribution of LNPs; a deeper channel with a higher aspect ratio promotes a more uniform LNP size.[48] The minimum size of LNPs generated by microfluidic devices is believed to be contingent upon the lipid-PEG content, which impedes the fusion of smaller LNPs.[31] An increased proportion of lipid-PEG content lowers the minimum achievable size, with the smallest reported LNP size being around 20 nm.[9]

2.3.2. Loading Efficiency. Loading efficiency is a critical determinant in LNP delivery systems, as it governs the lipid coassembly process during LNP formation.[49] This efficiency can be assessed by the weight ratio of lipid to mRNA or by the molar ratio of amino lipid nitrogen to nucleic acid phosphate (N/P). An enhanced loading efficiency can lead to a reduction in the required lipid dose, which is beneficial in minimizing overall toxicity, as excessive lipid intake may result in animal weight loss and even be lethal.[42] Nevertheless, it is not always advantageous to maximize nucleic acid loading, as LNPs with a lower N/P ratio may exhibit reduced positive charge at neutral pH, potentially impairing endosomal release.[13] For mRNA delivery, the optimized weight ratio between C12−200 and mRNA was10:1, with no significant change *in vivo* efficacy observed with increasing ionizable lipid ratio,[34] and a similar trend was also observed in the mRNA-LNP system composed of 5A2-SC8.[50] The N/P ratio has also been reported to significantly affect LNP morphology and charge status.[13]

2.3.3. Charges. The charge of LNPs is a critical parameter that significantly influences their transfection efficiency and *in vivo* delivery routes. The charge can be adjusted by manipulating the N/P ratio or by altering the chemical

https://doi.org/10.1021/acs.molpharmaceut.4c00925
Mol. Pharmaceutics 2025, 22, 1142−1159

properties of the lipid components. Increasing the positive charges of nanoparticles leads to the enhanced affinity toward anionic cellular membranes, potentially facilitating the cellular uptake and improve delivery efficiency. For example, LNPs with a reduced negative charge may exhibit greater *in vivo* potency following IM administration.[13] Adding permanent cationic lipid 1,2-Dioleoyl-3-trimethylammonium-propane (DOTAP) into LNP formulation also promoted the *in vitro* delivery efficiency of siRNA.[51]

Tailoring the LNP charge can achieve both cell-specific and tissue-specific targeting. Anionic LNPs, which are generated by replacing zwitterionic phospholipids with the anionic phospholipid 1,2-distearoyl-*sn*-glycero-3-phosphoglycerol (DSPG), display strong negative charges (zeta potential ∼ −20 mV) enabling preferential targeting to liver LSECs.[52] In addition, the selective Organ Targeting (SORT) strategy controls LNP charges by adding a fifth component (permanent cationic lipid, permanent anionic lipid, and ionizable lipid) to LNP, achieving targeted delivery to the lung, spleen, and liver.[53] In the lung SORT strategy, DOTAP was selected as the most effective permanent cationic lipid to formulate LNP for its superior transfection efficiency, high targeting specificity, and relatively low toxicity.[54] Lung SORT LNP assists in gene editing in multiple cell types in the lung including stem cells enabling long-term edits for 22 months.[55] Su et al. optimized the lung SORT strategy by developing a three-component LNP formulated by ionizable lipid, DOTAP, and PEG-lipid, showing the reduced accumulation in the liver and enhanced specificity to the lung potentially caused by the removal of cholesterol.[56] Additionally, spleen SORT LNP could deliver chimeric antigen receptor (CAR) mRNA to splenic T cells following IV injection to produce CAR T cells *in situ*.[57] Future optimization of the SORT LNP system could benefit from decreasing the off-targeted delivery, reducing the toxicity of SORT molecules, and exploring new target sites.

Zeta potential can detect the net charge of LNP, while pK_a may be used to evaluate the surface charge.[12] It is important to note that nonliver targeted LNPs often exhibit pK_a values which is out of the optimized pK_a range for hepatocyte delivery, highlighting the significant impact of LNP pK_a on delivery mechanisms. For instance, in the SORT system, lung-targeted LNPs display a higher pK_a (>9), while spleen-targeted LNPs have a lower pK_a (2−6,[58] 5.88−6.55[57]). The PEI-based LNP 7C1, designed for endothelial cell delivery, has a pK_a of approximately 5.0, which is lower than the typical pK_a range (6−7) established for liver delivery.[59] Low pK_a value has also been reported in spleen-targeted LNP systems formed by zwitterionic phospholipidated polymers.[60] Understanding the relationship between LNP pK_a and its targeted delivery could be essential for the guidance of future LNP targeting systems.

3. TARGETED LNP SYSTEM DESIGN

Designing targeted LNP systems is crucial for gene therapy, as it enables the specific and efficient delivery of therapeutic agents to designated cells or tissues within the body (as depicted in Figure 2). LNPs tend to accumulate in the liver even in the absence of specific targeting ligands, as studies have indicated that approximately 90% of standard LNPs are localized to the liver within 1 h post IV administration.[42] Targeted LNP strategies can lead to increased efficacy and reduced side effects compared to nontargeted delivery approaches. Various administration routes, including inhalation, intratumoral, intradermal, IV, and IM injections, significantly influence the targeting of LNPs to specific sites.[61] This section concentrates on the targeted delivery of LNPs facilitated by their intrinsic properties.

3.1. Active Targeting. Active targeting of LNPs is achieved through surface modification techniques. By conjugating targeting ligands to the LNP surface, these nanoparticles can be guided toward specific cell types, which fosters the advancement of targeted delivery platforms for a range of diseases. Targeting ligands, such as antibodies, sugars, and peptides, are typically attached to the distal end of PEGylated lipids or other polymeric lipids. This attachment facilitates direct interactions between the LNPs and the cell membrane without being shielded by the PEG layer.[62]

Antibody conjugation can achieve the targeted delivery to immune cells and stem cells. FIB504, a monoclonal antibody targeting the β7 integrin, was covalently attached to liposomes. Given the high expression of β7 integrin in gut mononuclear leukocytes, FIB504-modified LNPs were able to specifically target leukocytes, delivering siRNA to silence CyD1 and mitigate intestinal inflammation.[63] Anti-CD4 monoclonal antibody was chemically conjugated to LNPs, enabling specific siRNA delivery to $CD4^+$ T cells.[64] Their studies reveal that among leukocyte-rich organs (blood, spleen, lymph nodes, and bone marrow), the blood showed the highest LNP-cell binding affinity, while the lymph nodes exhibited the lowest binding. Anti-CD5-modified LNPs were utilized to deliver mRNA for the production of CAR T cells.[65] Additionally, LNPs covalently modified with anti-CD117 were found to effectively target hematopoietic stem cells (HSCs) in the bone marrow, offering a promising method for gene therapy for monogenic disorders and diseases affecting nonhematopoietic tissues.[66]

While conventional chemical conjugation strategies are widely utilized in LNP active targeting strategy, the binding efficacy could be compromised as the conjugated antibodies might be damaged during the chemical process. Additionally, chemically attached ligands are randomly oriented on the LNP surface, which means only a subset of them may be functional.[67] To address these limitations, the methodologies for targeted delivery have been developed, where bioactive ligands are attached to LNPs via noncovalent interactions. Dan Peer's laboratory pioneered the ASSET (Antibody-SS-Enabled Trigger) system, which allows for the conjugation of antibodies to LNPs through a recombinant protein approach.[67,68] In the ASSET system, the lipoprotein is a key component that contains a lipidation peptide domain for incorporation into LNPs and a scFv domain that interacts with the Fc region of the targeting antibody. The team also explored a supramolecular methodology using a secondary antibody as a linker between the LNP surface and the functional domain of the primary antibody, creating a conformation-sensitive targeting system.[69] This system allows integrin binding domains on LNPs to recognize integrin $\alpha4\beta7$ specifically in its high-affinity conformation.

Bioactive peptides have also emerged as cost-effective targeting ligands for LNP modification compared to antibodies. For example, a retina-specific peptide has been conjugated with a PEG-lipid of LNP, where the modified LNPs were capable of delivering mRNA to the neural retina, offering a promising therapeutic approach for treating inherited blindness.[70] Active targeting mechanisms can also be employed to achieve specific hepatic cell delivery within the liver. Standard LNPs, such as MC3, can be delivered to all major liver cell types, including hepatocytes, Kupffer cells (KCs), and hepatic

https://doi.org/10.1021/acs.molpharmaceut.4c00925
Mol. Pharmaceutics 2025, 22, 1142−1159

endothelial cells.[71] The engineering of LNP surfaces with N-acetylgalactosamine[27] and mannose[43] moieties has also been shown to enhance targeted delivery to hepatocytes and LSECs, respectively.

3.2. Passive Targeting. Active targeting mechanisms can enable cell-specific delivery systems for LNPs, but achieving tissue-specific delivery beyond the liver through the use of targeting ligand conjugation alone is challenging. Passive targeting mechanisms, on the other hand, can regulate tissue-specific targeting by adjusting the physicochemical properties of LNPs, potentially altering the protein corona. The delivery of classical LNPs to hepatocytes is facilitated by the interaction of apolipoprotein E (ApoE) with the low-density lipoprotein receptor (LDLr). LNPs typically form an ApoE-rich corona during circulation, which then binds to the LDLr that is abundantly expressed on hepatocyte surfaces.[72] It has been found that the corona of DOTAP-contained lung SORT LNP is enriched in vitronectin, leading to the increased uptake by lung cells that express the vitronectin receptor.[55]

It is worth noticing that the distinct surface chemistries of LNPs may lead to unique protein corona formations, and variations in the protein corona are thought to direct LNPs to different organs.[53] For example, LNPs based on the lipid 5A2-SC8 have shown high efficacy in targeting liver hepatocytes; however, minor alterations in lipid chemistry can result in the absence of ApoE in the protein corona, leading to delivery specificity for KCs instead.[73] Similarly, cationic LNPs[74] and anionic LNPs[72] have failed to target hepatocytes due to the lack of ApoE-based targeting.

4. APPLYING LNPS IN CRISPR/CAS GENE EDITING SYSTEMS

4.1. CRISPR/Cas Gene Editing Tools. CRISPR-Cas technology is revolutionizing the field of life sciences with its potentially transformative impact on biotechnology, agriculture, and medicine. Cas9 protein can cleave DNA in mammalian cells, creating double-strand breaks (DSBs) guided by CRISPR RNA in the presence of protospacer-adjacent motifs (PAMs).[75] Subsequently, it was successfully applied the CRISPR/Cas9 system for gene editing in human and mouse cells.[76] The CRISPR/Cas9 system consists of a sgRNA that directs the gene-editing machinery to the target DNA strand, with the Cas9 protein responsible for the DNA cleavage. DNA can be repaired primarily through nonhomologous end joining (NHEJ) or homology-directed repair (HDR) pathways.

CRISPR-Cas systems have been categorized into two classes, each further divided into six types and various subtypes, distinguished by their unique cas genes. Class 1 systems (types I, III, and IV) utilize multi-Cas protein complexes for interference, while class 2 systems (types II, V, and VI) achieve interference through a single effector protein. The effector proteins (Cas9, Cas12a, and Cas13) are involved in crRNA maturation in the three well-characterized examples of class 2 interference (type II, type V-A, and type VI), leading them to be prebound to the guide RNA before selecting and cleaving the target.[77] Cas13 proteins can be engineered for mammalian cell RNA knockdown and binding.[78] Based on CRISPR-Cas13, researchers have developed abundant of new RNA editing tools, including Cas13 nucleases,[79] REPAIR (RNA Editing for Programmable A to I Replacement)[80] and RESCUE (RNA Editing for Specific C-to-U Exchange)[81] RNA base editors, and RNA modification tools.

There are currently four classes of CRISPR-Cas-derived genome editing agents available for modifying genomes in experimental systems, including nucleases, base editors, transposases/recombinases, and prime editors (Table 1).

Table 1. Overview of Genome and Editing Strategies and Agents

Genetic edit	Edit type	Reagents/Methods
DNA	Stochastic indels	Cas9/Cas12 nucleases (DSB)
	PAM-distal transition point mutations	Base editors (ABEs, CBEs)
	PAM-proximal point mutations	Cas9/Cas12 nucleases (HDR) Prime editors
	Small insertions	Cas9/Cas12 nucleases (HDR) Prime editors
	Small deletions	Cas9/Cas12 nucleases (HDR) Prime editors
	Large insertions	Cas9/Cas12 nucleases (HDR/EJ) Cas transposases/recombinases
	Large deletions	Cas9/Cas12 nucleases (HDR/EJ)
	Chromosomal translocations	Cas9/Cas12 nucleases (HDR/EJ)
RNA	Transcript degradation	Cas13 nuclease
	Transcript point mutations	RNA base editors (REPAIR/RESCUE)

Some of these agents have quickly transitioned into clinical study. For example, the CRISPR-Cas9 system is widely used for producing nuclease-edited CAR-T cells.[82] Base editors (BEs) offer a solution to the limitations of nucleases by allowing precise gene correction through single-nucleotide conversions in genomic DNA without the need for DSB.[83] These BEs consist of DNA-modifying enzymes fused to programmable DNA-binding domains, and various types of BEs have been developed, including adenine base editors (ABE), cytosine base editors (CBE), and other types. BEs have been utilized in therapeutic settings for a variety of *ex vivo* and *in vivo* gene editing applications aimed at correcting disease-causing point mutations or introducing single-nucleotide variants to prevent or alleviate disease phenotypes.[84] Although BEs have the potential to correct most pathogenic single-nucleotide polymorphism (SNP), they are limited in their ability to perform all possible single-nucleotide conversions and cannot facilitate targeted insertions or deletions. In response to these constraints, prime editors (PEs) were developed allowing for the programmable installation of single-nucleotide conversion, small insertion, small deletion, or a combination thereof without creating DSB.[85] PEs consist of a reverse transcriptase fused to a Cas9 nickase domain and utilize an engineered prime editing guide RNA (pegRNA) to direct the Cas9 nickase to a specific target locus and encode the desired edit. The process involves nicking the nontarget DNA strand, priming reverse transcription using the pegRNA extension as a template, incorporating the desired edit into the newly synthesized strand, and biasing cellular DNA repair to replace the unedited strand with the edited strand. Multiple examples of *in vivo* gene editing using PEs have been documented.[84]

Gene editing agents can be introduced into cells through the delivery of pDNA or mRNA to encode their expression, or by directly administering proteins or RNPs. *In vivo* gene editing therapies hold the potential to address the underlying causes of

https://doi.org/10.1021/acs.molpharmaceut.4c00925
Mol. Pharmaceutics 2025, 22, 1142−1159

Table 2. Application of LNP in CRISPR/Cas Therapy

	Major lipid component of LNP	Size	Target gene	Cell type	Target tissue	Ref.
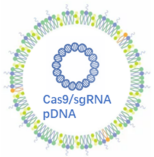	Ionizable lipid iLP181	~100 nm	*PLK1*	HEK293A; HepG2-Luc	Liver and tumor (IV injection); Tumor (intratumoral injection)	[104]
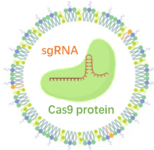 Cas9 RNP-LNP	Dendrimer 5A2-SC8; permanent cationic lipid DOTAP (lung targeting)	100-200 nm	LUC; GFP; STOP cassette; *PCSK9*	Hela-LUC; Hela-GFP	Muscle or brain (local injection); Liver or lung (IV injection)	[88]
	Bioreproducible lipid	74-292 nm	GFP	HEK-GFP	N/A	[90]
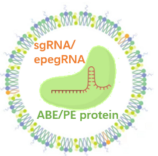 ABE/PE RNP-LNP	Ionizable lipid SM-102	194 nm	*RPE65*	*rd12* reporter cells	Retinal pigment epithelium (subretinal injection)	[89]
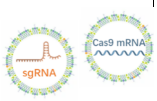 Cas9 mRNA-LNP & sgRNA-LNP	Cationic lipid TT3	N/A	GFP; *PCSK9*; HBV genome	Hepatocyte ; NIH3T3	Liver (IV injection)	[93]
	lipopeptide cKK-E12	N/A	GFP; *HBB; EXM1; PCSK9*;	HEK-GFP; Hepatocyte	Liver (IV injection)	[94]
	Ionizable lipid TCL053	~100 nm	*DMD*	Myoblast	Skeletal muscle (IM injection)	[105]
	Bioreproducible lipid	112 nm; 234 nm	GFP *PCSK9* STOP cassette; *ANGPTL3*	HEK-GFP; Hepatocyte	Liver (IV injection)	[21, 92]
 Cas9 mRNA-sgRNA-LNP	Zwitterionic amino lipid	70-200 nm	STOP cassette	Lung cancer cell	Liver, lung and kidney (IV injection)	[33]
	Ionizable lipid LP01	<100 nm	*TTR*	Hepatocyte	Liver (IV injection)	[19]
	Ionizable lipid 246C10	75 nm	*mAT*	Hepatocyte	Liver (IV injection)	[96]
	Ionizable lipid L8 (Anti-EGFR as target ligand)	71-80 nm	GFP; *PLK1*	HEK-GFP; GBM 005; OV8;	Tumor (intratumoral injection for unmodified LNP; intraperitoneal injection for modified LNP)	[101]

https://doi.org/10.1021/acs.molpharmaceut.4c00925
Mol. Pharmaceutics 2025, 22, 1142−1159

Table 2. continued

	Major lipid component of LNP	Size	Target gene	Cell type	Target tissue	Ref.
	Dendrimer 5A2-SC8; DODAP (liver targeting); permanent cationic lipid DOTAP (lung targeting); anionic lipid 18PA (spleen targeting)	<200 nm	STOP cassette; *PTEN; PCSK9*	N/A	Liver, lung and spleen (IV injection)	[53]
	Dendrimer 5A2-SC8; permanent cationic lipid DOTAP (lung targeting);	N/A	STOP cassette;	Diverse cell types in the lung	Lung (IV injection)	[55]
	Ionizable lipid (Clinic trail NTLA-2001)	N/A	*TTR*	Hepatocyte	Liver (IV injection)	[7]
	Lipid LP000001 (Clinic trail NTLA-2002)	N/A	*KLKB1*	Hepatocyte	Liver (IV injection)	[8]
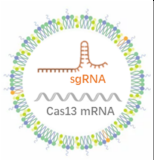 Cas13 mRNA-sgRNA-LNP	Ionizable lipid MC3; permanent cationic lipid DOTAP (lung targeting)	~100 nm	*CTSL*	HEK; Vero-ACE2-TMPRSS2; Caco-2	Lung (IV injection)	[99]
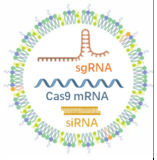 Cas9 mRNA-sgRNA-siRNA-LNP	Dendrimer 5A2-SC8	~120 nm	GFP; *PD-L1*	Hela-GFP; IGROV1; HepG2	Tumor (intratumoral injection)	[102]
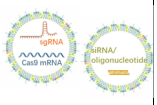 Cas9 mRNA-sgRNA-LNP& siRNA(oligonucleotide)-LNP	Polymer 7C1 (spleen or lung targeting) lipopeptide cKK-E12 (liver targeting)	~50 nm	GFP; *ICAM-2;*	Hepatocyte; Splenic or lung endothelial cells	Liver, lung, and spleen (IV injection)	[103]
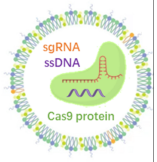	Ionizable lipid CL4H6	~200 nm	GFP; HBV genome	Hela-GFP; HEK-GFP; HBV-infected HepG2-hNTCP cell	N/A	[11]
Cas9 RNP-ssDNA-LNP	Ionizable lipid; Synthetic lipids derived from cholesterol	100-200 nm	GFP; *EMX1*; *AAVS1*; *CFTR*; STOP cassette; *PCSK9; SFTPC*	tdTOM NPCs; HEK-GFP; HBE	Liver and lung (IV injection)	[87]

https://doi.org/10.1021/acs.molpharmaceut.4c00925
Mol. Pharmaceutics 2025, 22, 1142−1159

Table 2. continued

	Major lipid component of LNP	Size	Target gene	Cell type	Target tissue	Ref.
	Dendrimer 4A3-SC8	~100 nm	GFP	HEK-GFP	Tumor (intratumoral injection)	91
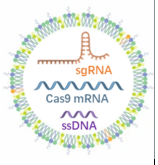 Cas9 mRNA-sgRNA-ssDNA-LNP	Dendrimer 5A2-SC8; permanent cationic lipid DOTAP (lung targeting)	~140 nm	GFP; *CFTR*	BFP/GFP switchable HEK293; Primary human bronchial epithelial cell	Lung (IV injection)	54
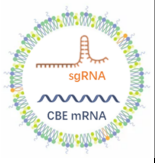 CBE mRNA-sgRNA-LNP	Ionizable lipid	67-71 nm	*PAH*	Hepatocyte	Liver (IV injection)	106
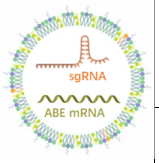 ABE mRNA-sgRNA-LNP	Ionizable lipid	95-105 nm; 65-71 nm	*PCSK9*	Hepatocyte	Liver (IV injection)	98, 100
	Dendrimer 5A2-SC8; permanent cationic lipid DOTAP (lung targeting)	90 nm (microfluidic system); 130 nm (vortex)	*CFTR*	Primary human bronchial epithelial cell; Lung stem cell	Lung (IV injection)	55
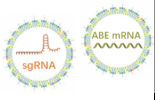 ABE mRNA-LNP & sgRNA-LNP	Ionizable lipid (Anti-CD117 as target ligand)	~80 nm	*E6V*	Sickle cell disease hematopoietic stem and progenitor cells	N/A	66

numerous genetic diseases if safe and effective target delivery methods are provided.

4.2. CRISPR/Cas Delivery Strategy Based on LNP. LNPs, initially designed and optimized for siRNA delivery, have gained recognition in CRISPR/Cas-based therapies where the cargo can be in the form of pDNA, mRNA, or RNP (Table 2). The delivery of the Cas9/sgRNA complex as an RNP complex is the most direct and rapid method for introducing the CRISPR/Cas machinery into cells. This approach is advantageous as it allows for transient expression, thereby minimizing off-target events compared to the use of DNA expression plasmids, due to the short intracellular half-life of RNPs.[86] The anionic nature of the RNP complex facilitates its coassembly with cationic lipids to form RNP-LNPs through electrostatic interactions. Furthermore, the inclusion of single-stranded oligonucleotides can enhance the stability of RNP-LNPs by increasing the negative charge density of the cargo.[11] However, the encapsulation of RNPs into LNPs can be challenging due to the potential denaturation of RNPs under acidic conditions. It can be addressed by optimizing the formulation[87] and the fabrication conditions (including pH and flow rate ratio in the microfluidic device)[11] to preserve the DNA cleavage activity of RNPs. SORT LNP also enables RNP encapsulation under neutral conditions by introducing permanent cationic lipid DOTAP into LNPs, where the structural integrity and biological function of RNPs are maintained.[88] Alternatively, ionizable lipid with pK_a above 6.0 can be utilized as the protonated lipid allowing RNP encapsulation at pH 6.0.[89] In addition to pH-responsive ionizable lipids, bioreproducible lipids have been utilized to formulate RNP-loaded LNPs as well, demonstrating low toxicity and high efficiency.[90]

An alternative strategy for CRISPR-Cas therapy involves the delivery of sgRNA and Cas9 in the form of mRNA, which also exhibits a low off-target rate due to the transient and nonintegrating nature of Cas9 expression.[21] The delivery of

https://doi.org/10.1021/acs.molpharmaceut.4c00925
Mol. Pharmaceutics 2025, 22, 1142−1159

Cas9 mRNA can produce a greater amount of protein compared to the direct delivery of the Cas9 protein in LNPs, potentially leading to higher potency.[91] For example, the use of bioreproducible LNPs for the delivery of Cas9 mRNA/sgRNA has higher genome knockout efficiency compared to the Cas9/sgRNA RNP complex.[92] Furthermore, Cas9 mRNA, Cas9 protein, and sgRNA delivered by LNPs can all be rapidly degraded *in vivo*, preventing long-term nuclease exposure.[93] Cas9 mRNA and sgRNA can be delivered by different approaches, as they can be encapsulated in a single nanoparticle (Cas9 mRNA-sgRNA-LNP) or delivered separately (Cas9 mRNA-LNP and sgRNA-LNP). It was found that administering sgRNA-LNP 6 h after Cas9 mRNA-LNP maximized the therapeutic effects, since it allows enough time for robust Cas9 protein expression.[93] However, recent studies have preferred the 'one-pot' strategy rather than the separate delivery, where the two cargos are more likely to be present in the same cell potentially result in higher *in vivo* efficacy.

Meanwhile, the delivery efficacy can also be improved by sgRNA modification, which will lead to higher indel rates when codelivered with Cas mRNA.[94] It is hypothesized that modified sgRNAs exhibit increased nuclease resistance, protecting them from degradation during Cas mRNA translation.[19,94] Once sgRNA binds to the Cas protein to form an RNP, the Cas protein can partially protect the sgRNA from degradation.[95] However, entrapping highly modified sgRNA in the classic approach could result in poor encapsulation efficiency due to the chemical environment change, and promoting the ionic strength in the aqueous phase during LNP fabrication could overcome this challenge.[96]

The HDR pathway, which requires an additional DNA template delivered alongside Cas9/sgRNA, has the advantage of causing fewer mutation errors. Anderson's lab previously combined viral and nonviral delivery methods to achieve HDR *in vivo*, with the sgRNA/repair template encoded in AAV and Cas9 mRNA delivered by LNP.[97] The 'one-pot' LNP delivery strategy, where the ssDNA template is incorporated into LNP together with RNP[11] or Cas9 mRNA/sgRNA cargo,[54,91] facilitates HDR as well. LNP platforms have also been successfully applied in base editor deliveries exhibiting accurate gene correction,[55,66,98,100,106] and RNA editing, where a CRISPR/Cas13d-based LNP therapy effectively suppresses *CTSL* mRNA expression.[99]

4.3. LNP Delivery of CRISPR/Cas for Gene Therapy. Given that many LNPs are intrinsically liver-targeted, they have the advantage of delivering gene-editing agents to treat hepatic diseases. For instance, CRISPR/Cas-LNP could target *PCSK9* gene for the treatment of familial hypercholesterolemia[98,100] and introduce indels into the Hepatitis B virus (HBV) DNA to suppress chronic HBV.[11,93] Liver-targeting CRISPR/Cas-LNP system has achieved high editing efficiency *in vivo* with minimal side effect. Delivery of ABE8.8 mRNA/sgRNA by LNP in cynomolgus monkey observed about 90% editing in *PCSK9* splice-site adenine and 60% reduction in low-density lipoprotein cholesterol.[98] The therapeutic efficacy of such liver-targeting treatments can provide durable genome editing for up to one year *in vivo*, with the potential for enhanced editing levels through repeated dosing.[19]

Combined with varied targeting delivery strategies, LNP-based gene editing has also been explored in extrahepatic tissue. Dan Peer's group designed a tumor-targeting LNP system by conjugating anti-EGFR to LNP through ASSET technology, where the modified LNP intraperitoneally delivered Cas9 mRNA/sgRNA to the tumor and achieved 82% editing in *PLK1*, effectively suppressing the tumor growth.[101] Siegwart's group designed a specialized LNP composed of three different nucleic acid cargos, with siRNA enhancing tissue penetration by reducing extracellular matrix stiffness and Cas9 mRNA/sgRNA editing the cancer-related genes.[102] Exploiting Lung SORT LNP technology in CRISPR/Cas system has shown promise in the treatment of SARS-CoV-2[99] and cystic fibrosis.[54,55] HSC-targeting LNP has been applied in ABE8e delivery for the treatment of sickle cell disease, leading to the high therapeutic editing rate (88%) *in vitro*, which significantly reduces the presence of sickled cells after erythroid differentiation.[66] IM delivery of LNPs allows for the treatment of muscular diseases, as a low-immunogenic LNP system has been developed for delivering Cas9 mRNA and a pair of sgRNAs to skeletal muscle, offering a promising therapeutic strategy for Duchenne muscular dystrophy.[6]

Though liver-targeting LNP gene therapy tends to exhibit high targeting specificity,[100] nonliver delivery systems could take off-target genome editing in unintended cells raising safety concern. For example, in the HSC-targeting LNP system, the off-target liver editing was over 70%.[66] Sago et al. developed an approach decreasing the off-target liver editing, which delivers siRNA and oligonucleotides via hepatocyte-targeted LNPs before delivering Cas9 mRNA/sgRNA to the lung or spleen. This approach silenced Cas9 mRNA and sgRNA in the liver, reducing off-target hepatocyte indels while maintaining gene editing efficiency in the lung or spleen.[103] More research is required in nonliver deliver systems to suppress off-target delivery.

Nowadays, the CRISPR/Cas-LNP system has obtained great success and several studies have moved into the clinic trail. NTLA-2001, the first LNP-based CRISPR/Cas clinic trail delivered by IV injection, was designed to treat transthyretin amyloidosis by knockout misfolded transthyretin (TTR) gene in hepatocytes.[7] The study reported that the decrease of TTR protein was detected in patient serum with only mild adverse effects 28 days after single-dose treatment. NTLA-2002 used CRISPR/Cas9 therapy to target *KLKB1* for the treatment of hereditary angioedema, leading to a reduction of total plasma kallikrein protein of 95% in high dose group without observed adverse events, and substantially decreased the frequency of angioedema attacks in patients.[8]

5. LNP OPTIMIZATION GUIDED BY MACHINE LEARNING

Machine learning techniques have significantly advanced research in biology, medicine, and pharmaceuticals by providing efficient alternatives to traditional experimental screening methods.[107] Unlike conventional approaches that often involve labor-intensive, time-consuming, and resource-demanding experiments, machine learning can handle high-dimensional and complex nonlinear data, automatically extracting key features from data sets. This capability allows researchers to analyze existing information and predict optimal outcomes, reducing reliance on extensive trial-and-error experimentation. As a result, machine learning contributes to faster, more efficient development processes while decreasing costs.[108]

The application of machine learning in LNP research has shown promise in improving drug delivery system development. Researchers focused on engineering safe and effective

https://doi.org/10.1021/acs.molpharmaceut.4c00925
Mol. Pharmaceutics 2025, 22, 1142−1159

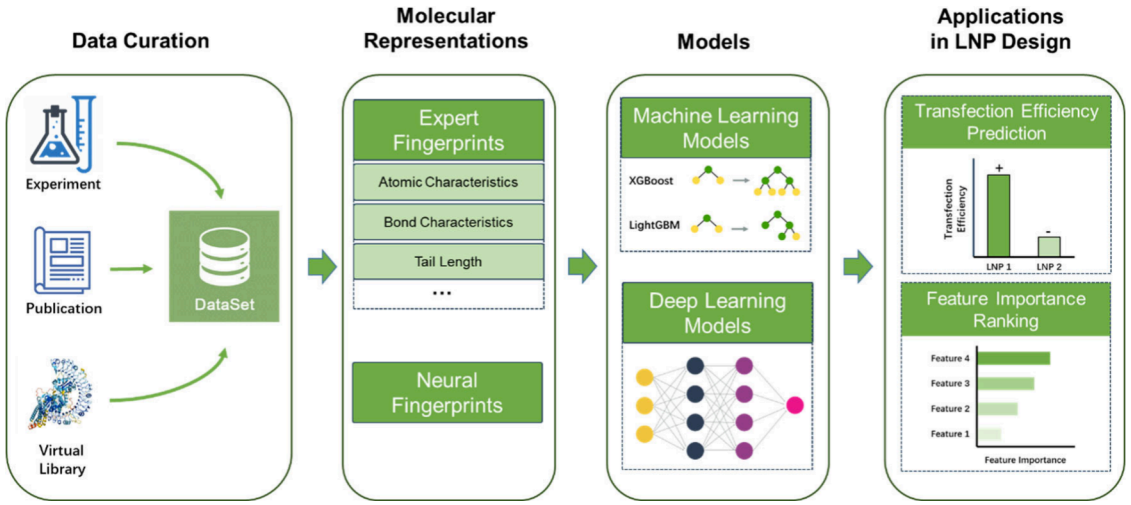

Figure 3. Overview of machine-learning guided LNP design.

LNP delivery systems primarily through the chemical modification of lipids and the adjustment of component ratios. However, the classical four-component LNP formulation can result in over 10^{10} distinct testable variations,[109] making the empirical screening excessively costly and time-intensive. In light of the application of machine learning in predicting and designing biomolecule properties in recent years, researchers have started to incorporate machine learning techniques in LNP research. This approach not only improves the accuracy of transfection efficiency predictions and refines nanoparticle design for therapeutic purposes, but also significantly reduces costs and shortens the development timeline.

A schematic representation of the research pipeline is presented in Figure 3.[110] This methodology encompasses several key steps (take the study of Li et al.[110] as an example): (1) Data collection, which involves acquiring data on LNPs formulated with 584 ionizable lipids from experimental procedures for model training; (2) Feature extraction, focusing on extracting the chemical features of the ionizable lipid of each LNP; (3) Data partitioning, where the 584 LNP data points are randomly divided into training and test sets, with the training set utilized for model training and the test set for assessing predictive accuracy and algorithm optimization; (4) Model application, employing the trained model to screen an extensive lipid library consisting of 40,000 lipids. This screening predicts optimal ionizable lipids, with the corresponding LNP delivery efficiency validated through *in vitro* and *in vivo* experiments. This machine learning approach facilitates the *in silico* screening of a vast molecular library, significantly accelerating the identification of highly effective molecules, such as ionizable lipids. This revolutionary methodology has attracted huge attention in the pharmaceutical industry. For instance, the biotechnology startup Mana.bio has introduced a platform that integrates artificial intelligence with LNP design.

5.1. Data Preparation for Machine Learning in LNP Research. The development of machine learning models for LNP research is facilitated by training data sourced from both wet-lab experiments and published papers. These data encompass the characteristics of LNPs, biological factors, and their corresponding potencies (e.g., transfection efficiency). To address the limited availability of public data sets for LNP research, innovative methodologies have been employed to generate and expand data sources. High-throughput experimental techniques have yielded substantial data sets in wet laboratories, as Cheng et al. reported 1080 outcomes of pDNA-LNP transfections across six different cell types,[111] and Li et al. tested the delivery efficiency of mRNA-LNP formulated by 584 different ionizable lipids.[110] In particular, Ugi combinatorial chemistry allows the multiple bond formation in a "one-pot" reaction, enabling the high-throughput synthesis of a large batch of ionizable lipids[112] and the formation of a vast and diverse molecular library. These extensive data sets provide a foundation for training machine learning models, where structure−activity relationships could be learned which improves the prediction accuracy. Additionally, the utilization of Ugi combinatorial chemistry assisted by ChemAxon's Marvin Suite with the Markush Editor (Marvin 23.4.0) has also been instrumental in expanding a virtual library.[113] The library is composed of 60,000 chemically diverse lipid structures with varied amine headgroups and alkyl chains.

Literature-derived data sets serve as an effective supplementary method, expanding the available data pool which typically includes hundreds to thousands of samples. Notable examples include a data set of 622 LNPs with detailed transfection efficiency information,[114] 325 LNP formulations designed for mRNA vaccine,[115] and an extensive data set of 2332 samples composed of analogous ALC-0315 and SM-102.[116] Different data, derived from both experimental and published sources, is essential for training and fine-tuning machine learning models. However, it is important to acknowledge that potential biases may arise when curating databases based on published studies, as transfection efficiencies from different studies may not be directly compared comprising the prediction accuracy. Data collected from wet-lab are more comparable due to the controllable experiment condition.[117]

5.2. Feature Presentation and Extraction in Machine Learning-Based LNP Studies. In the realm of machine learning-based LNP research, feature design is frequently contingent upon expert knowledge to enhance interpretability. These features delineate the molecular and structural characteristics of LNPs, encompassing a spectrum from atomic-level details to intricate molecular arrangements. They are essential for accurately modeling and forecasting the behavior and efficacy of LNPs. Table 3 encapsulates the

https://doi.org/10.1021/acs.molpharmaceut.4c00925
Mol. Pharmaceutics 2025, 22, 1142−1159

key features typically employed in such machine learning-driven LNP investigations.

Table 3. Typical Expert Features in Machine Learning-Based LNP Studies

Feature	Description
Atomic Types and Positions	Types and positions of atoms within a molecule, are foundational for understanding molecular composition.
Bond Types, Lengths, and Angles	Characteristics of chemical bonds are essential for defining molecular structure and geometry.
Lipid Tail Length and Structure	Tail length and structure of ionizable lipids, influencing stability and efficacy.
LNP Component Ratios	Ratios of components in LNPs are crucial for structural and functional integrity.
Functional Groups	Specific groups of atoms are responsible for characteristic chemical reactions.
Ring Structures	The presence and types of ring structures are significant for molecular stability and reactions.
Headgroup Structure	Specifics of ionizable lipid headgroup, affecting interaction with mRNA and transfection efficiency.
Ester Bonds	Positions and numbers of ester bonds within ionizable lipid molecules, influencing stability and biocompatibility.
Double Bonds	Influence of double bonds on molecular flexibility and reactivity.
Hydrophilicity and Hydrophobicity	Determination of molecular position in amphiphilic environments.
Surface Modifications	Target ligand modifications affecting LNP potency and biodistribution.
Encapsulation Efficiency	Efficiency of LNP to encapsulate nucleic acid cargo affecting stability and release rate.
Cell Lines	Types of cell lines used in *in vitro* experiments.

A detailed comprehension of the interplay between features and LNP behavior is essential for the advancement of more potent and secure delivery systems. In scenarios where data is scarce, expert knowledge assumes particular significance, as it bolsters the reliability and accuracy of predictive models. The integration of deep learning techniques for feature extraction with expert-informed features significantly amplifies the model's capacity to discern patterns and get insights from data.[113]

While expert knowledge-driven features play an important role in describing key LNP attributes, automated feature extraction methods are becoming increasingly important as data scales grow and molecular structures become more complex. Molecular descriptors such as SMILES (Simplified Molecular Input Line Entry System) and ECFP (extended-connectivity fingerprints) can automatically capture complex molecular structure information, providing rich input features for machine learning models. Molecular descriptors are essential tools that transform complex molecular structures into numerical forms that can be processed by machine learning models. In LNP research, using molecular descriptors allows for the automatic extraction of a wide range of structural features, reducing the reliance on manual feature engineering. SMILES is a linear notation system for representing chemical structures.[113] It encodes the atoms and bonds of a molecule into a string based on specific rules, allowing efficient processing of complex molecular structures by computers. Widely used in cheminformatics and machine learning, SMILES notation enables straightforward parsing and transformation into molecular graphs, where nodes represent atoms and edges represent bonds, supporting tasks like molecular property prediction.[118] ECFP descriptors are radial molecular fingerprints that capture local structures and connectivity within molecules.[115] ECFP works by iteratively recording information about each atom and its neighbors to generate a fixed-length numerical vector, effectively reflecting the structural characteristics of the molecule. Open-source cheminformatics tools such as RDKit can be used to process molecular descriptors, converting them into graph-based representations with nodes and edges that can be utilized for further model processing and learning. SMILES strings can be processed by RDKit to produce molecular representations, which are then transformed into atom graphs, providing the structural foundation for machine learning models to capture complex relationships between molecular structures and their biological activities.

For small-size data sets, expert knowledge-based features (often termed "expert fingerprints") might be favored as extensive research and experimentation have provided high confidence and good interpretability, thereby enhancing prediction accuracy. For larger data sets, deep learning-based methods utilizing molecular descriptors (referred to as "neural fingerprints") could be superior. Molecular descriptors have the potential to discover features that may not be easily captured by expert-driven approaches, learning more complex feature representations and effectively handling large-scale data. Combining molecular descriptors with expert features can complement each other to enhance the model's predictive power. For representation learning of LNP chemical information, molecular descriptors generated using identifiers like SMILES and ECFP are crucial for capturing and analyzing molecular structural features at a granular level, thereby enhancing the understanding of LNPs. This combined approach highlights the synergy between domain expertise and advanced pattern recognition capabilities, ultimately improving the predictive accuracy and reliability of machine learning models in LNP research.

5.3. Machine Learning Models in LNP Research. Multiple machine-learning models have been utilized to predict LNP delivery potency, demonstrating the versatility of computational techniques in this intricate field. These models are primarily based on supervised learning, trained using labeled data to predict specific LNP properties, such as transfection efficiency. Supervised learning is well-suited for tasks where there is a clear relationship between known features and labels.

Widely used machine learning models include Support Vector Machines (SVM), Random Forest algorithms, XGBoost, and Light Gradient Boosting Machine (LightGBM). SVMs, leveraging multiple kernel functions, are particularly effective for smaller data sets with high-dimensional features, allowing for the identification of optimal separating boundaries between classes. Random Forest algorithms are well-known for their capacity to handle high-dimensional data and capture complex nonlinear relationships among features providing feature importance rankings. XGBoost has used an ensemble of boosted trees to significantly enhance predictive accuracy, especially in handling imbalanced data sets. Similarly, decision tree-based models like LightGBM have also shown strong performance across various studies.[104,111,119] LightGBM is outstanding for its efficient handling of data sets, achieving accurate prediction with high computing speeding. MLPs, optimized with techniques like Adam, are also employed to learn complex mappings between input features and LNP

https://doi.org/10.1021/acs.molpharmaceut.4c00925
Mol. Pharmaceutics 2025, 22, 1142−1159

Table 4. Machine Learning Applied in Varied LNP Systems

LNP system	Training data source	Machine learning model	Validation	Application	Ref
mRNA-LNP vaccine	Published paper (325 samples)	LightGBM	*In vivo*	Predict the IgG titer of mRNA-LNP vaccine; Feature importance ranking and analysis.	115
siRNA-LNP	Published paper (129 *in vitro* formulations and 301 *in vivo* formulations)	LightGBM	*In vitro*	Predict the gene-knockdown efficiency of siRNA-LNP; Feature importance ranking and analysis.	122
mRNA-LNP	Published paper (2332 formulations across 14 publications)	LightGBM	*In vitro*	Predict the potency of LNP formulated by novel ionizable lipid	116
	Published paper (622 formulations)	SVM; Random forest; XGBoost; MLP	*In silico*	Predict the transfection efficiency of LNPs	114
	Virtual library (60000 lipids for self-supervised pretraining) & Wet-lab (1200 formulations for supervised fine-tuning)	Deep learning model	*In vitro* and *in vivo*	Present an AI-Guided Ionizable Lipid Engineering (AGILE) platform; Select the high-potent ionizable lipid for muscle injection and macrophage delivery	113
	Wet-lab (584 formulations)	Random forest; Logistic regression; XGBoost	*In vitro* and *in vivo*	Select the high-potent ionizable lipid; Feature importance ranking and analysis	110
pDNA-LNP	Wet-lab (180 formulations for 6 cell types)	Multiple linear regression; Lasso regression; Partial Least Squares regression; k-Nearest Neighbors Decision Trees; Random Forest; XGboost; LightGBM	*In silico*	Predict the transfection efficiency of LNPs; Feature importance ranking and analysis	111

properties. In machine learning models, especially in regression tasks, commonly used loss functions include Mean Squared Error (MSE) or Mean Absolute Error (MAE), as exemplified in the study conducted by Cheng et al.[111] These loss functions are used to measure the difference between the model's predicted values and the actual values, thereby guiding the training and optimization of the model.

Furthermore, the exploration of deep learning models represents a cutting-edge direction in LNP research. Multilayer Perceptrons (MLP), optimized using techniques such as Adam, are often employed as foundational models for learning complex mappings between input features and LNP properties. MLPs serve as a fundamental starting point in the application of deep learning, providing a straightforward yet powerful framework for approximating intricate relationships. Building on these foundational approaches, more sophisticated models based on Graph Neural Networks (GNN) have also been explored for their capability to capture the structural complexities of molecules. For instance, Li's group utilized the Graph Isomorphism Network (GIN) as an effective graph encoder to extract intricate features from molecular graphs.[110] GIN's proficiency in elucidating molecular structures through a nuanced understanding of nodes and edges highlights its applicability in domains requiring a comprehensive grasp of molecular configurations. In this work, GNNs were employed to extract molecular structural features of lipids, followed by an average pooling layer applied to each lipid molecular graph to produce a 512-dimensional lipid representation. This representation was then mapped to a 256-dimensional latent space using a single hidden layer MLP. Additionally, molecular descriptors calculated using Mordred[120] (over 1,000 common descriptors, including atom counts, bond counts, etc.) were mapped to a 100-dimensional latent vector through another MLP. These vectors were concatenated with the 256-dimensional lipid representations from the GNN encoder to form the final input feature vector. In the model pretraining phase, contrastive learning was adopted to learn a general representation of lipids by optimizing a contrastive loss function. The model parameters were initialized using the MolCLR model,[121] which was pretrained on over 10 million small molecules, providing a "warm start" and enhancing the model's learning capacity. After pretraining, the model was fine-tuned with an additional MLP, optimizing the loss function to improve predictive performance. During the contrastive learning stage, a contrastive loss function was used to learn LNP representations by contrasting positive data pairs against negative pairs. In the fine-tuning stage, MSE was used as the loss function for training, while Root Mean Squared Error (RMSE) was used for validation.

The vast search space presented by the chemical and compositional diversity of LNPs highlights the complexity involved in their design and optimization.[111,119] Deep learning models (GNNs in particular) have shown potential for predictive modeling in LNP research, yet they often rely on large and well-balanced data sets, which are scarce and frequently imbalanced in this domain. Few-shot learning could address these limitations, enabling effective model performance with limited data, while its adaptation to LNP applications is still evolving. In addition, many high-performing machine learning models operate as "black boxes" while the patterns driving the accurate predictions are still unclear.

5.4. Application of Machine Learning in LNP Systems.

Machine learning models have exhibited high prediction accuracy across various LNP systems which could be employed to screen the optimal LNP formulation *in silico*, and it can also effectively analyze feature importance and provide guidelines for LNP design, verifying the suitability of machine learning technique in LNP research (Table 4). Ouyang's group compiled LNP formulations and corresponding IgG or HAI titers from published literature to construct a machine-learning model for mRNA vaccine optimization.[115] The model's predictions were validated through *in vivo* testing. They also

https://doi.org/10.1021/acs.molpharmaceut.4c00925
Mol. Pharmaceutics 2025, 22, 1142−1159

applied machine learning to siRNA-LNP systems, where the model identified LNP dosage as the most critical feature influencing gene silencing performance both *in vitro* and *in vivo*.[122]

It has been observed that machine learning models can predict the performance of newly designed ionizable lipids not present in their training databases. The preferred physicochemical features of LNPs are found to vary across different cell types. Lewis et al. developed an ionizable lipid library consisting of analogs of SM-102 and ALC-0315, using a trained machine-learning model to predict transfection efficiency.[116] The predicted performance of novel ionizable lipids by the algorithm aligned with experimental results in the HEK293T cell line but not in A549. They also discovered that the tail length of ionizable lipids was the most influential chemical feature affecting mRNA transfection efficiency. AI-Guided Ionizable Lipid Engineering (AGILE) platform rapidly screened a pool of 12,000 novel ionizable lipids, where high-performance lipids selected from this process were tailored for IM injection and macrophage delivery.[113] It also found that for ionizable lipids, the headgroup structure significantly impacted LNP performance in HeLa cells, while the tail structure was the primary determinant of potency in RAW 264.7 cells. LNPs formulated with these selected high-performance ionizable lipids exhibited increased *in vitro* transfection efficiency and reduced off-target delivery compared to the benchmark MC3 lipid. Li et al. trained a machine learning model and screened a library of 40000 ionizable lipids in *silico*, where they selected the optimized ionizable lipid 119−23 exhibiting the outperformed delivery efficiency *in vitro* and *in vivo* compared to SM-102 and MC3 when formulating LNP.[110] With the assistance of Ugi combinatorial chemistry, machine learning might be employed to expertly develop the high-potent ionizable lipid with the lowest time cost.

6. CONCLUSION AND FUTURE PROSPECTS

The four-component LNP system has gained significant attention in gene therapy, offering potential for both disease treatment and prevention. Clinically advanced LNP formulations have shown efficient and safe delivery of nucleic acid payloads, facilitating repeat dosing over extended periods. Future iterations of LNP formulations are expected to enhance clinical performance further, with improvements anticipated in transfection efficiency and delivery specificity. The use of LNPs as carriers for CRISPR/Cas in gene therapy has been increasingly successful, with some studies progressing to clinical trials. However, the majority of CRISPR/Cas-lipid LNP systems are designed for liver and lung targeting, which leaves the targeting specificity for nonliver tissues comparatively lower. The specificity of nonliver-targeted LNP systems could be enhanced by curbing the undesired accumulation in the liver and by exploring novel targeting tissues beyond the liver and lung. This optimization may involve the development of innovative lipid formulations and a deeper understanding of the biodistribution patterns of LNPs *in vivo*. Integrating LNP-based CRISPR/Cas delivery with strategies for nonliver targeting is anticipated to expand the reach of gene editing therapies.

Machine learning holds significant potential to assist in the design and optimization of a variety of LNP systems. The application of machine leaning in LNP design could be hindered by the complex molecular structure, as large models require substantial computational resources. These challenges can be overcome by optimizing data-efficient techniques, enhancing model interpretability, and exploring scalable solutions. Leveraging large models with expert fine-tuning could combine general knowledge with targeted precision in LNP applications. Techniques such as generative models and diffusion-based approaches offer flexible frameworks supporting the innovation of LNP formulation.

While several studies have successfully employed trained machine learning models to predict the efficacy and assess the importance of various features, the application of machine learning in identifying optimal LNP formulations remains scarce. Concurrently, machine learning-based research has predominantly concentrated on enhancing delivery efficiency, with less emphasis on other critical aspects such as immunotoxicity and targeting specificity. It is important to broaden the scope of machine learning applications in LNP development to include a comprehensive evaluation of safety and targeting precision alongside efficiency.

AUTHOR INFORMATION

Corresponding Authors

Xingxu Huang − *The First Affiliated Hospital, Zhejiang University School of Medicine, Hangzhou, Zhejiang 311100, China*; Email: xingxuhuang@zju.edu.cn

Ming Li − *Department of Dermatology, Children's Hospital of Fudan University, National Children's Medical Center, Shanghai 201102, China*; Email: mingli@fudan.edu.cn

Yuan Yao − *ZJU-Hangzhou Global Scientific and Technological Innovation Canter, Zhejiang University, Hangzhou, Zhejiang 311215, China; College of Chemical and Biological Engineering, Zhejiang University, Hangzhou, Zhejiang 310027, China; Zhejiang Key Laboratory of Intelligent Manufacturing for Functional Chemicals, ZJU-Hangzhou Global Scientific and Technological Innovation Center, Zhejiang University, Hangzhou 311215, China*; orcid.org/0000-0001-5262-5115; Email: yyao1@zju.edu.cn

Authors

Yichen Yuan − *ZJU-Hangzhou Global Scientific and Technological Innovation Canter, Zhejiang University, Hangzhou, Zhejiang 311215, China; Research Center for Life Sciences Computing, Zhejiang Lab, Hangzhou, Zhejiang 311121, China*; orcid.org/0000-0002-6442-3470

Ying Li − *Research Center for Space Computing System, Zhejiang Lab, Hangzhou, Zhejiang 311121, China*

Guo Li − *ZJU-Hangzhou Global Scientific and Technological Innovation Canter, Zhejiang University, Hangzhou, Zhejiang 311215, China*

Liqun Lei − *The First Affiliated Hospital, Zhejiang University School of Medicine, Hangzhou, Zhejiang 311100, China*

Complete contact information is available at: https://pubs.acs.org/10.1021/acs.molpharmaceut.4c00925

Author Contributions

#Y. Yuan, Y. Li, G. Li, and L. Lei contributed equally to this work. Y. Y. organized this review. All authors contributed to the writing and editing of this paper.

Notes

The authors declare no competing financial interest.

https://doi.org/10.1021/acs.molpharmaceut.4c00925
Mol. Pharmaceutics 2025, 22, 1142−1159

■ ACKNOWLEDGMENTS

This work was partially supported by grants from the National Natural Science Foundation of China General Program (Grants 32071347, 32471372 to Yuan Yao), National Key R&D Program of China, the Ministry of Science and Technology (MOST) (Grants 2023YFC3402402 to Yuan Yao), ZJU-Hangzhou Global Scientific and Technological Innovation Center, Zhejiang University (Grants 02020200-K02013008 to Yuan Yao). And we acknowledge the support of the ZJU-Hangzhou Global Scientific and Technological Innovation Center, Zhejiang University, the iBiofoundary and the Core Facility of the Institute for Intelligent Bio/Chem Manufacturing.

■ REFERENCES

(1) Kuzmin, D. A.; Shutova, M. V.; Johnston, N. R.; Smith, O. P.; Fedorin, V. V.; Kukushkin, Y. S.; van der Loo, J. C. M.; Johnstone, E. C. The Clinical Landscape for Aav Gene Therapies. *Nat. Rev. Drug Discovery* **2021**, *20* (3), 173−174.

(2) Swiech, L.; Heidenreich, M.; Banerjee, A.; Habib, N.; Li, Y.; Trombetta, J.; Sur, M.; Zhang, F. In Vivo Interrogation of Gene Function in the Mammalian Brain Using Crispr-Cas9. *Nat. Biotechnol.* **2015**, *33* (1), 102−106.

(3) Raguram, A.; Banskota, S.; Liu, D. R. Therapeutic In vivo Delivery of Gene Editing Agents. *Cell* **2022**, *185* (15), 2806−2827.

(4) Sabnis, S.; Kumarasinghe, E. S.; Salerno, T.; Mihai, C.; Ketova, T.; Senn, J. J.; Lynn, A.; Bulychev, A.; McFadyen, I.; Chan, J.; et al. A Novel Amino Lipid Series for Mrna Delivery: Improved Endosomal Escape and Sustained Pharmacology and Safety in Non-Human Primates. *Mol. Ther.* **2018**, *26* (6), 1509−1519.

(5) Kon, E.; Ad-El, N.; Hazan-Halevy, I.; Stotsky-Oterin, L.; Peer, D. Targeting Cancer with Mrna−Lipid Nanoparticles: Key Considerations and Future Prospects. *Nat. Rev. Clin Oncol* **2023**, *20*, 739−754.

(6) Kenjo, E.; Hozumi, H.; Makita, Y.; Iwabuchi, K. A.; Fujimoto, N.; Matsumoto, S.; Kimura, M.; Amano, Y.; Ifuku, M.; Naoe, Y.; et al. Low Immunogenicity of Lnp Allows Repeated Administrations of Crispr-Cas9Mrna into Skeletal Muscle in Mice. *Nat. Commun.* **2021**, *12* (1), 7101.

(7) Gillmore, J.; Gane, E.; Taubel, J.; Kao, J.; Fontana, M.; Maitland Michael, L.; Seitzer, J.; O'Connell, D.; Walsh Kathryn, R.; Wood, K.; et al. Crispr-Cas9 in Vivo Gene Editing for Transthyretin Amyloidosis. *New Engl. J. Med.* **2021**, *385* (6), 493−502.

(8) Longhurst, H. J.; Lindsay, K.; Petersen, R. S.; Fijen, L. M.; Gurugama, P.; Maag, D.; Butler, J. S.; Shah, M. Y.; Golden, A.; Xu, Y.; et al. Crispr-Cas9 in Vivo Gene Editing of Klkb1 for Hereditary Angioedema. *New Engl. J. Med.* **2024**, *390* (5), 432−441.

(9) Belliveau, N. M.; Huft, J.; Lin, P. J.; Chen, S.; Leung, A. K.; Leaver, T. J.; Wild, A. W.; Lee, J. B.; Taylor, R. J.; Tam, Y. K.; et al. Microfluidic Synthesis of Highly Potent Limit-Size Lipid Nanoparticles for in Vivo Delivery of Sirna. *Mol. Ther Nucleic Acids* **2012**, *1* (8), e37.

(10) Chen, D.; Love, K. T.; Chen, Y.; Eltoukhy, A. A.; Kastrup, C.; Sahay, G.; Jeon, A.; Dong, Y.; Whitehead, K. A.; Anderson, D. G. Rapid Discovery of Potent Sirna-Containing Lipid Nanoparticles Enabled by Controlled Microfluidic Formulation. *J. Am. Chem. Soc.* **2012**, *134* (16), 6948−6951.

(11) Suzuki, Y.; Onuma, H.; Sato, R.; Sato, Y.; Hashiba, A.; Maeki, M.; Tokeshi, M.; Kayesh, M. E. H.; Kohara, M.; Tsukiyama-Kohara, K.; et al. Lipid Nanoparticles Loaded with Ribonucleoprotein−Oligonucleotide Complexes Synthesized Using a Microfluidic Device Exhibit Robust Genome Editing and Hepatitis B Virus Inhibition. *J. Controlled Release* **2021**, *330*, 61−71.

(12) Patel, P.; Ibrahim, N. M.; Cheng, K. The Importance of Apparent Pka in the Development of Nanoparticles Encapsulating Sirna and Mrna. *Trends Pharmacol. Sci.* **2021**, *42* (6), 448−460.

(13) Carrasco, M. J.; Alishetty, S.; Alameh, M.-G.; Said, H.; Wright, L.; Paige, M.; Soliman, O.; Weissman, D.; Cleveland, T. E.; Grishaev, A.; et al. Ionization and Structural Properties of Mrna Lipid Nanoparticles Influence Expression in Intramuscular and Intravascular Administration. *Commun. Biol.* **2021**, *4* (1), 956.

(14) Cullis, P. R.; Hope, M. J. Lipid Nanoparticle Systems for Enabling Gene Therapies. *Mol. Ther.* **2017**, *25* (7), 1467−1475.

(15) Whitehead, K. A.; Dorkin, J. R.; Vegas, A. J.; Chang, P. H.; Veiseh, O.; Matthews, J.; Fenton, O. S.; Zhang, Y.; Olejnik, K. T.; Yesilyurt, V.; et al. Degradable Lipid Nanoparticles with Predictable in Vivo Sirna Delivery Activity. *Nat. Commun.* **2014**, *5*, 4277.

(16) Semple, S. C.; Akinc, A.; Chen, J.; Sandhu, A. P.; Mui, B. L.; Cho, C. K.; Sah, D. W.; Stebbing, D.; Crosley, E. J.; Yaworski, E.; et al. Rational Design of Cationic Lipids for Sirna Delivery. *Nat. Biotechnol.* **2010**, *28* (2), 172−176.

(17) Jayaraman, M.; Ansell, S. M.; Mui, B. L.; Tam, Y. K.; Chen, J.; Du, X.; Butler, D.; Eltepu, L.; Matsuda, S.; Narayanannair, J. K.; et al. Maximizing the Potency of Sirna Lipid Nanoparticles for Hepatic Gene Silencing in Vivo. *Angew. Chem., Int. Ed.* **2012**, *51* (34), 8529−8533.

(18) Lam, K.; Leung, A.; Martin, A.; Wood, M.; Schreiner, P.; Palmer, L.; Daly, O.; Zhao, W.; McClintock, K.; Heyes, J. Unsaturated, Trialkyl Ionizable Lipids Are Versatile Lnp Components for Therapeutic and Vaccine Applications. *Adv. Mater.* **2023**, 2209624.

(19) Finn, J. D.; Smith, A. R.; Patel, M. C.; Shaw, L.; Youniss, M. R.; van Heteren, J.; Dirstine, T.; Ciullo, C.; Lescarbeau, R.; Seitzer, J.; et al. A Single Administration of Crispr/Cas9 Lipid Nanoparticles Achieves Robust and Persistent In vivo Genome Editing. *Cell Rep* **2018**, *22* (9), 2227−2235.

(20) Kim, T. I.; Kim, S. W. Bioreducible Polymers for Gene Delivery. *React. Funct. Polym.* **2011**, *71* (3), 344−349.

(21) Qiu, M.; Glass, Z.; Chen, J.; Haas, M.; Jin, X.; Zhao, X.; Rui, X.; Ye, Z.; Li, Y.; Zhang, F.; et al. Lipid Nanoparticle-Mediated Codelivery of Cas9Mrna and Single-Guide Rna Achieves Liver-Specific in Vivo Genome Editing of Angptl3. *Proc. Natl. Acad. Sci. U.S.A.* **2021**, *118* (10), e2020401118.

(22) Thévenot, J.; Troutier, A.-L.; David, L.; Delair, T.; Ladavière, C. Steric Stabilization of Lipid/Polymer Particle Assemblies by Poly(Ethylene Glycol)-Lipids. *Biomacromolecules* **2007**, *8* (11), 3651−3660.

(23) Zhang, Y.; Sun, C.; Wang, C.; Jankovic, K. E.; Dong, Y. Lipids and Lipid Derivatives for Rna Delivery. *Chem. Rev.* **2021**, *121* (20), 12181−12277.

(24) Lokugamage, M. P.; Vanover, D.; Beyersdorf, J.; Hatit, M. Z. C.; Rotolo, L.; Echeverri, E. S.; Peck, H. E.; Ni, H.; Yoon, J.-K.; Kim, Y.; et al. Optimization of Lipid Nanoparticles for the Delivery of Nebulized Therapeutic Mrna to the Lungs. *Nat. Biomed. Eng.* **2021**, *5* (9), 1059−1068.

(25) Ambegia, E.; Ansell, S.; Cullis, P.; Heyes, J.; Palmer, L.; MacLachlan, I. Stabilized Plasmid−Lipid Particles Containing Peg-Diacylglycerols Exhibit Extended Circulation Lifetimes and Tumor Selective Gene Expression. *Biochim. Biophys. Acta* **2005**, *1669* (2), 155−163.

(26) Mok, K. W. C.; Lam, A. M. I.; Cullis, P. R. Stabilized Plasmid-Lipid Particles: Factors Influencing Plasmid Entrapment and Transfection Properties. *Biochim. Biophys. Acta* **1999**, *1419* (2), 137−150.

(27) Chen, S.; Tam, Y. Y. C.; Lin, P. J. C.; Leung, A. K. K.; Tam, Y. K.; Cullis, P. R. Development of Lipid Nanoparticle Formulations of Sirna for Hepatocyte Gene Silencing Following Subcutaneous Administration. *J. Controlled Release* **2014**, *196*, 106−112.

(28) Kulkarni, J. A.; Witzigmann, D.; Leung, J.; Tam, Y. Y. C.; Cullis, P. R. On the Role of Helper Lipids in Lipid Nanoparticle Formulations of Sirna. *Nanoscale* **2019**, *11* (45), 21733−21739.

(29) Krause, M. R.; Regen, S. L. The Structural Role of Cholesterol in Cell Membranes: From Condensed Bilayers to Lipid Rafts. *Acc. Chem. Res.* **2014**, *47* (12), 3512−3521.

(30) Douka, S.; Brandenburg, L. E.; Casadidio, C.; Walther, J.; Garcia, B. B. M.; Spanholtz, J.; Raimo, M.; Hennink, W. E.; Mastrobattista, E.; Caiazzo, M. Lipid Nanoparticle-Mediated Mes-

senger Rna Delivery for Ex Vivo Engineering of Natural Killer Cells. *J. Controlled Release* **2023**, *361*, 455−469.
(31) Kulkarni, J. A.; Darjuan, M. M.; Mercer, J. E.; Chen, S.; van der Meel, R.; Thewalt, J. L.; Tam, Y. Y. C.; Cullis, P. R. On the Formation and Morphology of Lipid Nanoparticles Containing Ionizable Cationic Lipids and Sirna. *ACS Nano* **2018**, *12* (5), 4787−4795.
(32) Li, Z.; Carter, J.; Santos, L.; Webster, C.; van der Walle, C. F.; Li, P.; Rogers, S. E.; Lu, J. R. Acidification-Induced Structure Evolution of Lipid Nanoparticles Correlates with Their in Vitro Gene Transfections. *ACS Nano* **2023**, *17* (2), 979−990.
(33) Miller, J. B.; Zhang, S.; Kos, P.; Xiong, H.; Zhou, K.; Perelman, S. S.; Zhu, H.; Siegwart, D. J. Non-Viral Crispr/Cas Gene Editing in Vitro and in Vivo Enabled by Synthetic Nanoparticle Co-Delivery of Cas9Mrna and Sgrna. *Angew. Chem., Int. Ed. Engl.* **2017**, *56* (4), 1059−1063.
(34) Kauffman, K. J.; Dorkin, J. R.; Yang, J. H.; Heartlein, M. W.; DeRosa, F.; Mir, F. F.; Fenton, O. S.; Anderson, D. G. Optimization of Lipid Nanoparticle Formulations for Mrna Delivery in Vivo with Fractional Factorial and Definitive Screening Designs. *Nano Lett.* **2015**, *15* (11), 7300−7306.
(35) Liu, S.; Cheng, Q.; Wei, T.; Yu, X.; Johnson, L. T.; Farbiak, L.; Siegwart, D. J. Membrane-Destabilizing Ionizable Phospholipids for Organ-Selective Mrna Delivery and Crispr−Cas Gene Editing. *Nat. Mater.* **2021**, *20* (5), 701−710.
(36) Maurer, N.; Wong, K. F.; Stark, H.; Louie, L.; McIntosh, D.; Wong, T.; Scherrer, P.; Semple, S. C.; Cullis, P. R. Spontaneous Entrapment of Polynucleotides Upon Electrostatic Interaction with Ethanol-Destabilized Cationic Liposomes. *Biophys. J.* **2001**, *80* (5), 2310−2326.
(37) Jeffs, L. B.; Palmer, L. R.; Ambegia, E. G.; Giesbrecht, C.; Ewanick, S.; MacLachlan, I. A Scalable, Extrusion-Free Method for Efficient Liposomal Encapsulation of Plasmid DNA. *Pharm. Res.* **2005**, *22* (3), 362−372.
(38) Thorsen, T.; Roberts, R. W.; Arnold, F. H.; Quake, S. R. Dynamic Pattern Formation in a Vesicle-Generating Microfluidic Device. *Phys. Rev. Lett.* **2001**, *86* (18), 4163−4166. Anna, S. L.; Bontoux, N.; Stone, H. A. Formation of Dispersions Using "Flow Focusing" in Microchannels. *Appl. Phys. Lett.* **2003**, *82* (3), 364−366.
(39) Jahn, A.; Vreeland, W. N.; Gaitan, M.; Locascio, L. E. Controlled Vesicle Self-Assembly in Microfluidic Channels with Hydrodynamic Focusing. *J. Am. Chem. Soc.* **2004**, *126* (9), 2674−2675.
(40) Zook, J. M.; Vreeland, W. N. Effects of Temperature, Acyl Chain Length, and Flow-Rate Ratio on Liposome Formation and Size in a Microfluidic Hydrodynamic Focusing Device. *Soft Matter* **2010**, *6* (6), 1352−1360.
(41) Hunter, M. R.; Cui, L.; Porebski, B. T.; Pereira, S.; Sonzini, S.; Odunze, U.; Iyer, P.; Engkvist, O.; Lloyd, R. L.; Peel, S.; et al. Understanding Intracellular Biology to Improve Mrna Delivery by Lipid Nanoparticles. *Small Methods* **2023**, *7*, 2201695.
(42) Akinc, A.; Goldberg, M.; Qin, J.; Dorkin, J. R.; Gamba-Vitalo, C.; Maier, M.; Jayaprakash, K. N.; Jayaraman, M.; Rajeev, K. G.; Manoharan, M.; et al. Development of Lipidoid-Sirna Formulations for Systemic Delivery to the Liver. *Mol. Ther.* **2009**, *17* (5), 872−879.
(43) Kim, M.; Jeong, M.; Hur, S.; Cho, Y.; Park, J.; Jung, H.; Seo, Y.; Woo, H. A.; Nam, K. T.; Lee, K.; et al. Engineered Ionizable Lipid Nanoparticles for Targeted Delivery of Rna Therapeutics into Different Types of Cells in the Liver. *Sci. Adv.* **2021**, *7* (9), eabf4398.
(44) Perrault, S. D.; Walkey, C.; Jennings, T.; Fischer, H. C.; Chan, W. C. W. Mediating Tumor Targeting Efficiency of Nanoparticles through Design. *Nano Lett.* **2009**, *9* (5), 1909−1915.
(45) Chen, S.; Tam, Y. Y. C.; Lin, P. J. C.; Sung, M. M. H.; Tam, Y. K.; Cullis, P. R. Influence of Particle Size on the in Vivo Potency of Lipid Nanoparticle Formulations of Sirna. *J. Controlled Release* **2016**, *235*, 236−244.
(46) Tsoi, K. M.; MacParland, S. A.; Ma, X.-Z.; Spetzler, V. N.; Echeverri, J.; Ouyang, B.; Fadel, S. M.; Sykes, E. A.; Goldaracena, N.; Kaths, J. M.; et al. Mechanism of Hard-Nanomaterial Clearance by The liver. *Nat. Mater.* **2016**, *15* (11), 1212−1221.
(47) Terada, T.; Kulkarni, J. A.; Huynh, A.; Chen, S.; van der Meel, R.; Tam, Y. Y. C.; Cullis, P. R. Characterization of Lipid Nanoparticles Containing Ionizable Cationic Lipids Using Design-of-Experiments Approach. *Langmuir* **2021**, *37* (3), 1120−1128.
(48) Jahn, A.; Vreeland, W. N.; DeVoe, D. L.; Locascio, L. E.; Gaitan, M. Microfluidic Directed Formation of Liposomes of Controlled Size. *Langmuir* **2007**, *23* (11), 6289−6293.
(49) Li, S.; Hu, Y.; Li, A.; Lin, J.; Hsieh, K.; Schneiderman, Z.; Zhang, P.; Zhu, Y.; Qiu, C.; Kokkoli, E.; et al. Payload Distribution and Capacity of Mrna Lipid Nanoparticles. *Nat. Commun.* **2022**, *13* (1), 5561.
(50) Cheng, Q.; Wei, T.; Jia, Y.; Farbiak, L.; Zhou, K.; Zhang, S.; Wei, Y.; Zhu, H.; Siegwart, D. J. Dendrimer-Based Lipid Nanoparticles Deliver Therapeutic Fah Mrna to Normalize Liver Function and Extend Survival in a Mouse Model of Hepatorenal Tyrosinemia Type I. *Adv. Mater.* **2018**, *30* (52), e1805308.
(51) He, Y.; Bi, D.; Plantinga, J. A.; Molema, G.; Bussmann, J.; Kamps, J. A. A. M. Development of a Combined Lipid-Based Nanoparticle Formulation for Enhanced Sirna Delivery to Vascular Endothelial Cells. *Pharmaceutics* **2022**, *14* (10), 2086.
(52) Pattipeiluhu, R.; Arias-Alpizar, G.; Basha, G.; Chan, K. Y. T.; Bussmann, J.; Sharp, T. H.; Moradi, M.-A.; Sommerdijk, N.; Harris, E. N.; Cullis, P. R.; et al. Anionic Lipid Nanoparticles Preferentially Deliver Mrna to the Hepatic Reticuloendothelial System. *Adv. Mater.* **2022**, *34* (16), e2201095.
(53) Cheng, Q.; Wei, T.; Farbiak, L.; Johnson, L. T.; Dilliard, S. A.; Siegwart, D. J. Selective Organ Targeting (Sort) Nanoparticles for Tissue-Specific Mrna Delivery and Crispr−Cas Gene Editing. *Nat. Nanotechnol* **2020**, *15* (4), 313−320.
(54) Wei, T.; Sun, Y.; Cheng, Q.; Chatterjee, S.; Traylor, Z.; Johnson, L. T.; Coquelin, M. L.; Wang, J.; Torres, M. J.; Lian, X.; et al. Lung Sort Lnps Enable Precise Homology-Directed Repair Mediated Crispr/Cas Genome Correction in Cystic Fibrosis Models. *Nat. Commun.* **2023**, *14* (1), 7322.
(55) Sun, Y.; Chatterjee, S.; Lian, X.; Traylor, Z.; Sattiraju, S. R.; Xiao, Y.; Dilliard, S. A.; Sung, Y.-C.; Kim, M.; Lee, S. M.; et al. In Vivo Editing of Lung Stem Cells for Durable Gene Correction in Mice. *Science* **2024**, *384* (6701), 1196−1202.
(56) Su, K.; Shi, L.; Sheng, T.; Yan, X.; Lin, L.; Meng, C.; Wu, S.; Chen, Y.; Zhang, Y.; Wang, C.; et al. Reformulating Lipid Nanoparticles for Organ-Targeted Mrna Accumulation and Translation. *Nat. Commun.* **2024**, *15* (1), 5659.
(57) Álvarez-Benedicto, E.; Tian, Z.; Chatterjee, S.; Orlando, D.; Kim, M.; Guerrero, E. D.; Wang, X.; Siegwart, D. J. Spleen Sort Lnp Generated in Situ Car T Cells Extend Survival in a Mouse Model of Lymphoreplete B Cell Lymphoma. *Angew. Chem., Int. Ed.* **2023**, *62* (44), e202310395.
(58) Dilliard, S. A.; Cheng, Q.; Siegwart, D. J. On the Mechanism of Tissue-Specific Mrna Delivery by Selective Organ Targeting Nanoparticles. *Proc. Natl. Acad. Sci. U.S.A.* **2021**, *118* (52), e2109256118.
(59) Dahlman, J. E.; Barnes, C.; Khan, O.; Thiriot, A.; Jhunjunwala, S.; Shaw, T. E.; Xing, Y.; Sager, H. B.; Sahay, G.; Speciner, L.; et al. In Vivo Endothelial Sirna Delivery Using Polymeric Nanoparticles with Low Molecular Weight. *Nat. Nanotechnol* **2014**, *9* (8), 648−655.
(60) Liu, S.; Wang, X.; Yu, X.; Cheng, Q.; Johnson, L. T.; Chatterjee, S.; Zhang, D.; Lee, S. M.; Sun, Y.; Lin, T.-C.; et al. Zwitterionic Phospholipidation of Cationic Polymers Facilitates Systemic Mrna Delivery to Spleen and Lymph Nodes. *J. Am. Chem. Soc.* **2021**, *143* (50), 21321−21330.
(61) Hou, X.; Zaks, T.; Langer, R.; Dong, Y. Lipid Nanoparticles for Mrna Delivery. *Nature Reviews Materials* **2021**, *6* (12), 1078−1094. Xu, X.; Xia, T. Recent Advances in Site-Specific Lipid Nanoparticles for Mrna Delivery. *ACS Nanoscience Au* **2023**, *3* (3), 192−203.
(62) Torchilin, V. P.; Rammohan, R.; Weissig, V.; Levchenko, T. S. Tat Peptide on the Surface of Liposomes Affords Their Efficient Intracellular Delivery Even at Low Temperature and in the Presence of Metabolic Inhibitors. *Proc. Natl. Acad. Sci. U. S. A.* **2001**, *98* (15), 8786−8791.

https://doi.org/10.1021/acs.molpharmaceut.4c00925
Mol. Pharmaceutics 2025, 22, 1142−1159

(63) Peer, D.; Park, E. J.; Morishita, Y.; Carman, C. V.; Shimaoka, M. Systemic Leukocyte-Directed Sirna Delivery Revealing Cyclin D1 as an Anti-Inflammatory Target. *Science* **2008**, *319* (5863), 627−630.
(64) Ramishetti, S.; Kedmi, R.; Goldsmith, M.; Leonard, F.; Sprague, A. G.; Godin, B.; Gozin, M.; Cullis, P. R.; Dykxhoorn, D. M.; Peer, D. Systemic Gene Silencing in Primary T Lymphocytes Using Targeted Lipid Nanoparticles. *ACS Nano* **2015**, *9* (7), 6706−6716.
(65) Rurik, J. G.; Tombácz, I.; Yadegari, A.; Méndez Fernández, P. O.; Shewale, S. V.; Li, L.; Kimura, T.; Soliman, O. Y.; Papp, T. E.; Tam, Y. K.; et al. Car T Cells Produced in Vivo to Treat Cardiac Injury. *Science* **2022**, *375* (6576), 91−96.
(66) Breda, L.; Papp, T. E.; Triebwasser, M. P.; Yadegari, A.; Fedorky, M. T.; Tanaka, N.; Abdulmalik, O.; Pavani, G.; Wang, Y.; Grupp, S. A.; et al. In Vivo Hematopoietic Stem Cell Modification by Mrna Delivery. *Science* **2023**, *381* (6656), 436−443.
(67) Kedmi, R.; Veiga, N.; Ramishetti, S.; Goldsmith, M.; Rosenblum, D.; Dammes, N.; Hazan-Halevy, I.; Nahary, L.; Leviatan-Ben-Arye, S.; Harlev, M.; et al. A Modular Platform for Targeted Rnai Therapeutics. *Nat. Nanotechnol* **2018**, *13* (3), 214−219.
(68) Veiga, N.; Goldsmith, M.; Granot, Y.; Rosenblum, D.; Dammes, N.; Kedmi, R.; Ramishetti, S.; Peer, D. Cell Specific Delivery of Modified Mrna Expressing Therapeutic Proteins to Leukocytes. *Nat. Commun.* **2018**, *9* (1), 4493.
(69) Dammes, N.; Goldsmith, M.; Ramishetti, S.; Dearling, J. L. J.; Veiga, N.; Packard, A. B.; Peer, D. Conformation-Sensitive Targeting of Lipid Nanoparticles for Rna Therapeutics. *Nat. Nanotechnol* **2021**, *16* (9), 1030−1038.
(70) Herrera-Barrera, M.; Ryals, R. C.; Gautam, M.; Jozic, A.; Landry, M.; Korzun, T.; Gupta, M.; Acosta, C.; Stoddard, J.; Reynaga, R.; et al. Peptide-Guided Lipid Nanoparticles Deliver Mrna to the Neural Retina of Rodents and Nonhuman Primates. *Sci. Adv.* **2023**, *9* (2), eadd4623.
(71) Sago, C. D.; Lokugamage, M. P.; Islam, F. Z.; Krupczak, B. R.; Sato, M.; Dahlman, J. E. Nanoparticles That Deliver Rna to Bone Marrow Identified by in Vivo Directed Evolution. *J. Am. Chem. Soc.* **2018**, *140* (49), 17095−17105.
(72) Yan, X.; Kuipers, F.; Havekes, L. M.; Havinga, R.; Dontje, B.; Poelstra, K.; Scherphof, G. L.; Kamps, J. A. The Role of Apolipoprotein E in the Elimination of Liposomes from Blood by Hepatocytes in the Mouse. *Biochem. Biophys. Res. Commun.* **2005**, *328* (1), 57−62.
(73) Johnson, L. T.; Zhang, D.; Zhou, K.; Lee, S. M.; Liu, S.; Dilliard, S. A.; Farbiak, L.; Chatterjee, S.; Lin, Y.-H.; Siegwart, D. J. Lipid Nanoparticle (Lnp) Chemistry Can Endow Unique in Vivo Rna Delivery Fates within the Liver That Alter Therapeutic Outcomes in a Cancer Model. *Mol. Pharmaceutics* **2022**, *19* (11), 3973−3986.
(74) Akinc, A.; Querbes, W.; De, S.; Qin, J.; Frank-Kamenetsky, M.; Jayaprakash, K. N.; Jayaraman, M.; Rajeev, K. G.; Cantley, W. L.; Dorkin, J. R.; et al. Targeted Delivery of Rnai Therapeutics with Endogenous and Exogenous Ligand-Based Mechanisms. *Mol. Ther.* **2010**, *18* (7), 1357−1364.
(75) Jinek, M.; Chylinski, K.; Fonfara, I.; Hauer, M.; Doudna, J. A.; Charpentier, E. A Programmable Dual-Rna−Guided DNA Endonuclease in Adaptive Bacterial Immunity. *Science* **2012**, *337* (6096), 816−821.
(76) Cong, L.; Ran, F. A.; Cox, D.; Lin, S.; Barretto, R.; Habib, N.; Hsu, P. D.; Wu, X.; Jiang, W.; Marraffini, L. A.; et al. Multiplex Genome Engineering Using Crispr/Cas Systems. *Science* **2013**, *339* (6121), 819−823.
(77) Makarova, K. S.; Haft, D. H.; Barrangou, R.; Brouns, S. J. J.; Charpentier, E.; Horvath, P.; Moineau, S.; Mojica, F. J. M.; Wolf, Y. I.; Yakunin, A. F.; et al. Evolution and Classification of the Crispr−Cas Systems. *Nat. Rev. Microbiol* **2011**, *9* (6), 467−477.
(78) Abudayyeh, O. O.; Gootenberg, J. S.; Essletzbichler, P.; Han, S.; Joung, J.; Belanto, J. J.; Verdine, V.; Cox, D. B. T.; Kellner, M. J.; Regev, A.; et al. Rna Targeting with Crispr−Cas13. *Nature* **2017**, *550* (7675), 280−284.
(79) Hillary, V. E.; Ceasar, S. A. A Review on the Mechanism and Applications of Crispr/Cas9/Cas12/Cas13/Cas14 Proteins Utilized for Genome Engineering. *Mol. Biotechnol.* **2023**, *65* (3), 311−325.
(80) Cox, D. B. T.; Gootenberg, J. S.; Abudayyeh, O. O.; Franklin, B.; Kellner, M. J.; Joung, J.; Zhang, F. Rna Editing with Crispr-Cas13. *Science* **2017**, *358* (6366), 1019−1027.
(81) Abudayyeh, O. O.; Gootenberg, J. S.; Franklin, B.; Koob, J.; Kellner, M. J.; Ladha, A.; Joung, J.; Kirchgatterer, P.; Cox, D. B. T.; Zhang, F. A Cytosine Deaminase for Programmable Single-Base Rna Editing. *Science* **2019**, *365* (6451), 382−386.
(82) Eyquem, J.; Mansilla-Soto, J.; Giavridis, T.; van der Stegen, S. J. C.; Hamieh, M.; Cunanan, K. M.; Odak, A.; Gönen, M.; Sadelain, M. Targeting a Car to the Trac Locus with Crispr/Cas9 Enhances Tumour Rejection. *Nature* **2017**, *543* (7643), 113−117.
(83) Gaudelli, N. M.; Komor, A. C.; Rees, H. A.; Packer, M. S.; Badran, A. H.; Bryson, D. I.; Liu, D. R. Programmable Base Editing of a•T to G•C in Genomic DNA without DNA Cleavage. *Nature* **2017**, *551* (7681), 464−471.
(84) Newby, G. A.; Liu, D. R. In vivo Somatic Cell Base Editing and Prime Editing. *Mol. Ther.* **2021**, *29* (11), 3107−3124.
(85) Anzalone, A. V.; Randolph, P. B.; Davis, J. R.; Sousa, A. A.; Koblan, L. W.; Levy, J. M.; Chen, P. J.; Wilson, C.; Newby, G. A.; Raguram, A.; et al. Search-and-Replace Genome Editing without Double-Strand Breaks or Donor DNA. *Nature* **2019**, *576* (7785), 149−157.
(86) Banskota, S.; Raguram, A.; Suh, S.; Du, S. W.; Davis, J. R.; Choi, E. H.; Wang, X.; Nielsen, S. C.; Newby, G. A.; Randolph, P. B.; et al. Engineered Virus-Like Particles for Efficient In vivo Delivery of Therapeutic Proteins. *Cell* **2022**, *185* (2), 250−265.
(87) Chen, K.; Han, H.; Zhao, S.; Xu, B.; Yin, B.; Lawanprasert, A.; Trinidad, M.; Burgstone, B. W.; Murthy, N.; Doudna, J. A. Lung and Liver Editing by Lipid Nanoparticle Delivery of a Stable Crispr−Cas9 Ribonucleoprotein. *Nat. Biotechnol.* **2024**, DOI: 10.1038/s41587-024-02437-3.
(88) Wei, T.; Cheng, Q.; Min, Y.-L.; Olson, E. N.; Siegwart, D. J. Systemic Nanoparticle Delivery of Crispr-Cas9 Ribonucleoproteins for Effective Tissue Specific Genome Editing. *Nat. Commun.* **2020**, *11* (1), 3232.
(89) Hołubowicz, R.; Du, S. W.; Felgner, J.; Smidak, R.; Choi, E. H.; Palczewska, G.; Menezes, C. R.; Dong, Z.; Gao, F.; Medani, O. Safer and Efficient Base Editing and Prime Editing Via Ribonucleoproteins Delivered through Optimized Lipid-Nanoparticle Formulations. *Nat. Biomed. Eng.* **2024**, DOI: 10.1038/s41551-024-01296-2.
(90) Wang, M.; Zuris, J. A.; Meng, F.; Rees, H.; Sun, S.; Deng, P.; Han, Y.; Gao, X.; Pouli, D.; Wu, Q.; et al. Efficient Delivery of Genome-Editing Proteins Using Bioreducible Lipid Nanoparticles. *Proc. Natl. Acad. Sci. U. S. A.* **2016**, *113* (11), 2868−2873. Li, Y.; Yang, T.; Yu, Y.; Shi, N.; Yang, L.; Glass, Z.; Bolinger, J.; Finkel, I. J.; Li, W.; Xu, Q. Combinatorial Library of Chalcogen-Containing Lipidoids for Intracellular Delivery of Genome-Editing Proteins. *Biomaterials* **2018**, *178*, 652−662.
(91) Farbiak, L.; Cheng, Q.; Wei, T.; Álvarez-Benedicto, E.; Johnson, L. T.; Lee, S.; Siegwart, D. J. All-in-One Dendrimer-Based Lipid Nanoparticles Enable Precise Hdr-Mediated Gene Editing in Vivo. *Adv. Mater.* **2021**, *33* (30), 2006619.
(92) Liu, J.; Chang, J.; Jiang, Y.; Meng, X.; Sun, T.; Mao, L.; Xu, Q.; Wang, M. Fast and Efficient Crispr/Cas9 Genome Editing in Vivo Enabled by Bioreducible Lipid and Messenger Rna Nanoparticles. *Adv. Mater.* **2019**, *31* (33), e1902575.
(93) Jiang, C.; Mei, M.; Li, B.; Zhu, X.; Zu, W.; Tian, Y.; Wang, Q.; Guo, Y.; Dong, Y.; Tan, X. A Non-Viral Crispr/Cas9 Delivery System for Therapeutically Targeting Hbv DNA and Pcsk9 in Vivo. *Cell Res.* **2017**, *27* (3), 440−443.
(94) Yin, H.; Song, C. Q.; Suresh, S.; Wu, Q.; Walsh, S.; Rhym, L. H.; Mintzer, E.; Bolukbasi, M. F.; Zhu, L. J.; Kauffman, K.; et al. Structure-Guided Chemical Modification of Guide Rna Enables Potent Non-Viral in Vivo Genome Editing. *Nat. Biotechnol.* **2017**, *35* (12), 1179−1187.

(95) Hendel, A.; Bak, R. O.; Clark, J. T.; Kennedy, A. B.; Ryan, D. E.; Roy, S.; Steinfeld, I.; Lunstad, B. D.; Kaiser, R. J.; Wilkens, A. B.; et al. Chemically Modified Guide Rnas Enhance Crispr-Cas Genome Editing in Human Primary Cells. *Nat. Biotechnol.* **2015**, *33* (9), 985−989.
(96) Han, J. P.; Kim, M.; Choi, B. S.; Lee, J. H.; Lee, G. S.; Jeong, M.; Lee, Y.; Kim, E.-A.; Oh, H.-K.; Go, N.; et al. In Vivo Delivery of Crispr-Cas9 Using Lipid Nanoparticles Enables Antithrombin Gene Editing for Sustainable Hemophilia a and B Therapy. *Sci. Adv.* **2022**, *8* (3), eabj6901.
(97) Yin, H.; Song, C. Q.; Dorkin, J. R.; Zhu, L. J.; Li, Y.; Wu, Q.; Park, A.; Yang, J.; Suresh, S.; Bizhanova, A.; et al. Therapeutic Genome Editing by Combined Viral and Non-Viral Delivery of Crispr System Components in Vivo. *Nat. Biotechnol.* **2016**, *34* (3), 328−333.
(98) Musunuru, K.; Chadwick, A. C.; Mizoguchi, T.; Garcia, S. P.; DeNizio, J. E.; Reiss, C. W.; Wang, K.; Iyer, S.; Dutta, C.; Clendaniel, V.; et al. In Vivo Crispr Base Editing of Pcsk9 Durably Lowers Cholesterol in Primates. *Nature* **2021**, *593* (7859), 429−434.
(99) Cui, Z.; Zeng, C.; Huang, F.; Yuan, F.; Yan, J.; Zhao, Y.; Zhou, Y.; Hankey, W.; Jin, V. X.; Huang, J.; et al. Cas13d Knockdown of Lung Protease Ctsl Prevents and Treats Sars-Cov-2 Infection. *Nat. Chem. Biol.* **2022**, *18* (10), 1056−1064.
(100) Rothgangl, T.; Dennis, M. K.; Lin, P. J. C.; Oka, R.; Witzigmann, D.; Villiger, L.; Qi, W.; Hruzova, M.; Kissling, L.; Lenggenhager, D.; et al. In Vivo Adenine Base Editing of Pcsk9 in Macaques Reduces Ldl Cholesterol Levels. *Nat. Biotechnol.* **2021**, *39* (8), 949−957.
(101) Rosenblum, D.; Gutkin, A.; Kedmi, R.; Ramishetti, S.; Veiga, N.; Jacobi, A. M.; Schubert, M. S.; Friedmann-Morvinski, D.; Cohen, Z. R.; Behlke, M. A.; et al. Crispr-Cas9 Genome Editing Using Targeted Lipid Nanoparticles for Cancer Therapy. *Sci. Adv.* **2020**, *6* (47), eabc9450.
(102) Zhang, D.; Wang, G.; Yu, X.; Wei, T.; Farbiak, L.; Johnson, L. T.; Taylor, A. M.; Xu, J.; Hong, Y.; Zhu, H.; et al. Enhancing Crispr/Cas Gene Editing through Modulating Cellular Mechanical Properties for Cancer Therapy. *Nat. Nanotechnol* **2022**, *17* (7), 777−787.
(103) Sago, C. D.; Lokugamage, M. P.; Loughrey, D.; Lindsay, K. E.; Hincapie, R.; Krupczak, B. R.; Kalathoor, S.; Sato, M.; Echeverri, E. S.; Fitzgerald, J. P.; et al. Augmented Lipid-Nanoparticle-Mediated in Vivo Genome Editing in the Lungs and Spleen by Disrupting Cas9 Activity in the Liver. *Nat. Biomed. Eng.* **2022**, *6* (2), 157−167.
(104) Li, C.; Yang, T.; Weng, Y.; Zhang, M.; Zhao, D.; Guo, S.; Hu, B.; Shao, W.; Wang, X.; Hussain, A.; et al. Ionizable Lipid-Assisted Efficient Hepatic Delivery of Gene Editing Elements for Oncotherapy. *Bioact. Mater.* **2022**, *9*, 590−601.
(105) Kenjo, E.; Hozumi, H.; Makita, Y.; Iwabuchi, K. A.; Fujimoto, N.; Matsumoto, S.; Kimura, M.; Amano, Y.; Ifuku, M.; Naoe, Y.; et al. Low Immunogenicity of Lnp Allows Repeated Administrations of Crispr-Cas9Mrna into Skeletal Muscle in Mice. *Nat. Commun.* **2021**, *12* (1), 7101.
(106) Villiger, L.; Rothgangl, T.; Witzigmann, D.; Oka, R.; Lin, P. J. C.; Qi, W.; Janjuha, S.; Berk, C.; Ringnalda, F.; Beattie, M. B.; et al. In Vivo Cytidine Base Editing of Hepatocytes without Detectable Off-Target Mutations in Rna and DNA. *Nat. Biomed. Eng.* **2021**, *5* (2), 179−189.
(107) Ekins, S.; Puhl, A. C.; Zorn, K. M.; Lane, T. R.; Russo, D. P.; Klein, J. J.; Hickey, A. J.; Clark, A. M. Exploiting Machine Learning for End-to-End Drug Discovery and Development. *Nat. Mater.* **2019**, *18* (5), 435−441. Peteani, G.; Huynh, M. T. D.; Gerebtzoff, G.; Rodríguez-Pérez, R. Application of Machine Learning Models for Property Prediction to Targeted Protein Degraders. *Nat. Commun.* **2024**, *15* (1), 5764. Ham, D. T.; Browne, T. S.; Banglorewala, P. N.; Wilson, T. L.; Michael, R. K.; Gloor, G. B.; Edgell, D. R. A Generalizable Cas9/Sgrna Prediction Model Using Machine Transfer Learning with Small High-Quality Datasets. *Nat. Commun.* **2023**, *14* (1), 5514.
(108) Mirza, B.; Wang, W.; Wang, J.; Choi, H.; Chung, N. C.; Ping, P. Machine Learning and Integrative Analysis of Biomedical Big Data. *Genes* **2019**, *10*, 87. Greener, J. G.; Kandathil, S. M.; Moffat, L.; Jones, D. T. A Guide to Machine Learning for Biologists. *Nat. Rev. Mol. Cell Biol.* **2022**, *23* (1), 40−55.
(109) Lokugamage, M. P.; Sago, C. D.; Dahlman, J. E. Testing Thousands of Nanoparticles In vivo Using DNA Barcodes. *Curr. Opin. Biomed. Eng.* **2018**, *7*, 1−8.
(110) Li, B.; Raji, I. O.; Gordon, A. G. R.; Sun, L.; Raimondo, T. M.; Oladimeji, F. A.; Jiang, A. Y.; Varley, A.; Langer, R. S.; Anderson, D. G. Accelerating Ionizable Lipid Discovery for Mrna Delivery Using Machine Learning and Combinatorial Chemistry. *Nat. Mater.* **2024**, *23* (7), 1002−1008.
(111) Cheng, L.; Zhu, Y.; Ma, J.; Aggarwal, A.; Toh, W. H.; Shin, C.; Sangpachatanaruk, W.; Weng, G.; Kumar, R.; Mao, H. Q. Machine Learning Elucidates Design Features of Plasmid DNA Lipid Nanoparticles for Cell Type-Preferential Transfection. *ACS Nano* **2024**, *18* (42), 28735−28747.
(112) Miao, L.; Li, L.; Huang, Y.; Delcassian, D.; Chahal, J.; Han, J.; Shi, Y.; Sadtler, K.; Gao, W.; Lin, J.; et al. Delivery of Mrna Vaccines with Heterocyclic Lipids Increases Anti-Tumor Efficacy by Sting-Mediated Immune Cell Activation. *Nat. Biotechnol.* **2019**, *37* (10), 1174−1185.
(113) Xu, Y.; Ma, S.; Cui, H.; Chen, J.; Xu, S.; Wang, K.; Varley, A.; Lu, R.; Wang, B.; Li, B. Agile Platform: A Deep Learning-Powered Approach to Accelerate Lnp Development for Mrna Delivery. *Nat. Commun.* **2024**, *15*, 6305.
(114) Ding, D. Y.; Zhang, Y.; Jia, Y.; Sun, J. Machine Learning-Guided Lipid Nanoparticle Design for Mrna Delivery. *arxiv:2308.01402* **2023**, DOI: 10.48550/arXiv.2308.01402.
(115) Wang, W.; Feng, S.; Ye, Z.; Gao, H.; Lin, J.; Ouyang, D. Prediction of Lipid Nanoparticles for Mrna Vaccines by the Machine Learning Algorithm. *Acta Pharm. Sin. B* **2022**, *12* (6), 2950−2962.
(116) Lewis, M.; Beck, T.; Ghosh, D. Applying Machine Learning to Identify Ionizable Lipids for Nanoparticle-Mediated Delivery of Mrna. *bioRxiv: 2023.2011.2009.565872* **2023**, DOI: 10.1101/2023.11.09.565872.
(117) van der Meel, R.; Grisoni, F.; Mulder, W. J. M. Lipid Discovery for Mrna Delivery Guided by Machine Learning. *Nat. Mater.* **2024**, *23* (7), 880−881.
(118) Moayedpour, S.; Broadbent, J.; Riahi, S.; Bailey, M.; V. Thu, H.; Dobchev, D.; Balsubramani, A.; N.D. Santos, R.; Kogler-Anele, L.; Corrochano-Navarro, A.; et al. Representations of Lipid Nanoparticles Using Large Language Models for Transfection Efficiency Prediction. *Bioinformatics* **2024**, *40* (7), btae342.
(119) Zhu, Y.; Shen, R.; Vuong, I.; Reynolds, R. A.; Shears, M. J.; Yao, Z.-C.; Hu, Y.; Cho, W. J.; Kong, J.; Reddy, S. K.; et al. Multi-Step Screening of DNA/Lipid Nanoparticles and Co-Delivery with Sirna to Enhance and Prolong Gene Expression. *Nat. Commun.* **2022**, *13* (1), 4282.
(120) Yang, L.; Gong, L.; Wang, P.; Zhao, X.; Zhao, F.; Zhang, Z.; Li, Y.; Huang, W. Recent Advances in Lipid Nanoparticles for Delivery of Mrna. *Pharmaceutics* **2022**, *14* (12), 2682.
(121) Wang, Y.; Wang, J.; Cao, Z.; Barati Farimani, A. Molecular Contrastive Learning of Representations Via Graph Neural Networks. *Nat. Mach. Intell* **2022**, *4* (3), 279−287.
(122) Gao, H.; Kan, S.; Ye, Z.; Feng, Y.; Jin, L.; Zhang, X.; Deng, J.; Chan, G.; Hu, Y.; Wang, Y.; et al. Development of in Silico Methodology for Sirna Lipid Nanoparticle Formulations. *Chem. Eng. J.* **2022**, *442*, 136310.